CDT
Centre de
Développement
Technologique
École Polytechnique
de Montréal

CDT PROJECT P971

-- FINAL REPORT --

DEVELOPMENT OF A SOLID STATE ARSENIC PROBE FOR USE IN PYROMETALLURGICAL PROCESSES

prepared for:

J.M. Skeaff
Contract # OST84-00339
CANMET, Energy, Mines & Ressources Canada
555, Booth Street
Ottawa (Ontario) K1A 0G1

by:

J. Kirchnerova
C.W. Bale
Department of Metallurgical Engineering
Ecole Polytechnique de Montréal

submitted by:

LE CENTRE DE DÉVELOPPEMENT TECHNOLOGIQUE
DE L'ECOLE POLYTECHNIQUE DE MONTREAL
Campus de l'Université de Montréal
Case postale 6079, Succursale A
Montréal (Québec) H3C 3A7

September 1986

MICROMEDIA

126 pp

J. Kirchnerova

C.W. Bale
Project Director

CDT
Centre de Développement Technologique
École Polytechnique de Montréal

92-04562/

TABLE OF CONTENTS

		Page
TABLE OF CONTENTS		i
LIST OF TABLES		iii
LIST OF FIGURES		iv
TABLES IN APPENDIX		viii
1.	SUMMARY	1
2.	BACKGROUND	4
3.	OBJECTIVE	6
4.	ANALYSIS OF THE PROBLEM	7
	4.1 Arsenic Oxides	9
	4.2 Solid Electrolytes	13
	4.3 Reference Electrodes	17
	4.4 Design of the Sensor	19
	4.5 Selectivity and Range of Application	20
	4.5.1 An arsenic oxide sensor for pyrometallurgical processes	20
	4.5.2 Galvanic cell for the determination of the thermodynamic properties of several base metal (Cu, Co, Ni, Fe) arsenates	22
5.	EXPERIMENTAL	23
	5.1 Gases	23
	5.2 Solid Electrolytes	24
	5.3 Cell Assembly	26
	5.4 Temperature Control	28
	5.5 Temperature and EMF Measurements	28
6.	RESULTS AND DISCUSSION	29
	6.1 Evaluation of the $AgZr_2(AsO_4)_3$ Electrolyte	30
	6.2 Evaluation of the $NaCaAsO_4$ Electrolyte	33
	6.3 Evaluation of the Ag-β-alumina Electrolyte	38
	6.3.1 Activity of silver in the electrolyte	41
	6.3.2 Initial sensor equilibration with arsine - formation of Ag_3AsO_4 on the surface	42
	6.3.3 Response time	42
	6.3.4 Gas Flowrates	43
	6.3.5 Reproducibility	43

TABLE OF CONTENTS

		Page
6.3.6	EMF as a function of P_{AsH_3} or $\tilde{P}_{As_4O_6}$ at P_{O_2} = 0.21 atm	44
6.3.5.1	Sensor I	44
6.3.6.2a	Sensor II - sensitivity to arsine	44
6.3.6.2b	Sensor II - sensitivity to arsenic oxide generated by an arsenolite bath	45
6.3.7	EMF as a function of P_{O_2} at P_{AsH_3} = const	45
6.3.7.1	Sensor I	45
6.3.7.2	Sensor II	46
6.3.8	EMF as a function of temperature	47
6.3.8.1	Sensor I	47
6.3.8.2	Sensor II	48
6.3.8.3	Sensor II-2	49
6.3.9	Interpretation of experimental results	50
6.4	Evaluation of the Na-β-alumina Electrolyte	58
6.4.1	Air as a reference electrode	59
6.4.2	Initial sensor equilibration with arsenic trioxide or arsine	59
6.4.3	Response time	60
6.4.4	Gas Flowrates	60
6.4.5	Reproducibility	61
6.4.6	EMF as a function of P_{AsH_3} at P_{O_2} = 0.21 atm	61
6.4.7	EMF as a function of P_{O_2} at P_{AsH_3} = const	62
6.4.8	EMF as a function of temperature	62
6.4.9	Interpretation of the results	62
7.	CONCLUSIONS	66
8.	SUGGESTIONS FOR FUTHER WORK	68
9.	REFERENCES	70

CDT
Centre de
Développement
Technologique
École Polytechnique
de Montréal

LIST OF TABLES

Page

Table 1: Solid electrolytes potentially suitable as arsenic oxide sensors 14

Table 2: Properties of silver and sodium arsenates 16

Table 3: Thermal properties of Ag_3SO_4 and Ag_3ASO_4 21

Table 4: Conditions for the synthesis of solid electrolytes 25

Table 5: Values of EMF [6.2.4] - EMF [6.2.3] 37

Table 6: Values of the slope b for the functions

EMF = a + b log P_{O_2} (for $P_{O_2} \to 1$) 47

Table 7: Gas concentrations and flowrates for measurements of EMF as a function of temperature 48

Table 8: Values of the parameters a and b in the equation [6.3.27] and corresponding ΔH°_{Rx} values and estimates of ΔG°_{Rx1000} for the cells [6.3.1] and [6.3.2] 56

Table 9: Estimates of ΔG°_{Rx} values for the reaction of the cells [6.3.1] and [6.3.2] 57

Table 10: Estimates of $\Delta G^\circ_{Na\text{-}ars.}$ values for the reactions of the cell [6.4.1] 65

LIST OF FIGURES

		Page
Figure 1:	Potentiometric sensor for use with solid electrolyte pellets	76
Figure 2:	Experimental assembly with a potentiometric sensor comprising a solid electrolyte closed-end tube	77
Figure 2a:	Sensor I with the reference on the outside	77
Figure 2b:	Sensor II with the reference on the inside	77
Figure 2c:	Complete assembly	77
Figure 3:	Gas mixing train	78
Figure 4:	Arsenolite saturator	79
Figure 5:	X-ray spectra of the prepared solid electrolytes	80
Figure 6:	EMF as a function of log $P_{AsH_3} P_{O_2}^2$ [P = atm] for the $AgZr_2(AsO_4)_3$ electrolyte at 985°K. The different points correspond to different days of measurement and/or to different flowrates	81
Figure 7:	EMF as a function of log $P_{AsH_3} P_{O_2}^5$ [P = atm] for the $NaCaAsO_4$ electrolyte at 949°, 1017° and 1075°K. Reference gas concentration: $\tilde{P}_{As_4O_6}$ = 1.3 ppm and P_{O_2} = 0.21 atm. Gas mixtures prepared by mixing arsine/nitrogen with either oxygen or air.	82
Figure 8:	EMF as a function of log $P_{AsH_3} P_{O_2}^3$ [P = atm] for the $NaCaAsO_4$ electrolyte at 949°, 1017° and 1075°K. Reference gas concentration: $\tilde{P}_{As_4O_6}$ = 1.3 ppm and P_{O_2} = 0.21 atm. Gas mixtures prepared by mixing arsine/nitrogen with either oxygen or air.	83
Figure 9:	EMF as a function of log P_{AsH_3} [atm] for the Ag β-alumina electrolyte, sensor I, at 986°, 1008°, 1118°, 1124° and 1174° K and P_{O_2} = 0.21 atm	84

LIST OF FIGURES

Page

Figure 10: EMF as a function of log P_{AsH_3} [atm] for the Ag β-alumina electrolyte, sensor II, at 974°K and P_{O_2} = 0.21 atm: Flowrate: 0.5 ml/s 85

Figure 11: EMF as a function of log P_{O_2} [atm] for the Ag β-alumina electrolyte, sensor I, at P_{AsH_3} = 5.3 ppm and 986°, 1008° and 1124°K 86

Figure 12: EMF as a function of log P_{O_2} [atm] for the Ag β-alumina electrolyte, sensor I, at P_{AsH_3} = 23 ppm and 986°, 1008°, 1124° and 1173°K 87

Figure 13: EMF as a function of log P_{O_2} [atm] for the Ag β-alumina electrolyte, sensor I, for P_{AsH_3} = 255 ppm at 986°, 1008°, 1032° and 1173°K 88

Figure 14: EMF as a function of log P_{O_2} [atm] for the Ag β-alumina electrolyte, sensor II, for P_{AsH_3} = 5.3 ppm at 924° and 974°K, and for P_{AsH_3} = 266 ppm and 1007°K 89

Figure 15: EMF as a function of temperature for Ag β-alumina electrolyte, sensor I:

a) sensor I, P_{AsH_3} = 1847 ppm, P_{O_2} = 0.63 atm, flowrate (f.r.) = 0.15 ml/s: ■) heating, □) cooling 90-91

b) sensor I, P_{AsH_3} = 255 ppm, P_{O_2} = 0.95 atm, f.r. = 1 ml/s, heating 90-91

c) sensor I, P_{AsH_3} = 36 ppm, P_{O_2} = 0.63 atm, f.r. = 0.6 ml/s: ▲) heating, ○ , ▽) cooling 90-91

d) sensor I, P_{AsH_3} = 255 ppm, P_{O_2} = 0.21 atm, f.r. = 1 ml/s, cooling 90-91

LIST OF FIGURES

Page

Figure 16: EMF as a function of temperature for the Ag β-alumina electrolyte, sensor II: e) P_{AsH_3} = 1847 ppm, P_{O_2} = 0.63 atm, flowrate = 0.15 ml/s; f) P_{AsH_3} = 36 ppm, P_{O_2} = 0.63 atm, flowrate 1 ml/s 92

Figure 17: EMF as a function of temperature for the Ag β-alumina electrolyte, sensor II-2, $\tilde{P}_{As_4O_6}$ = 31.1 ppm, P_{O_2} = 0.21 atm, flowrate 0.5 ml/s □) heating, o) cooling 93

Figure 18: EMF/T values as a function of 1/T for the Ag β-alumina electrolyte:

a) sensor I, P_{AsH_3} = 1847 ppm, P_{O_2} = 0.63 atm, flowrate = 0.15 ml/s 94-95

b) sensor I, P_{AsH_3} = 255 ppm, P_{O_2} = 0.95 atm, f.r. = 1 ml/s 94-95

c) sensor I, P_{AsH_3} = 36 ppm, P_{O_2} = 0.63 atm, f.r. = 0.6 ml/s 94-95

d) sensor I, P_{AsH_3} = 255 ppm, P_{O_2} = 0.21 atm, f.r. = 1 ml/s 94-95

e) sensor II, P_{AsH_3} = 1847 ppm, P_{O_2} = 0.63 atm, f.r. = 0.15 ml/s 94-95

f) sensor II, P_{AsH_3} = 36 ppm, P_{O_2} = 0.63 atm, f.r. = 0.6 ml/s 94-95

g) sensor II-2, $\tilde{P}_{As_4O_6}$ = 31.1 ppm, P_{O_2} = 0.21 atm, f.r. = 0.5 ml/s 94-95

LIST OF FIGURES

Page

Figure 19: EMF as a function of log P_{AsH_3} [atm] for the sodium β-alumina electrolyte with air as a reference: at 1025°K, △) first set of data, ▲) second set of data; at 1075°K, □) first set, ○) second set of data 96

Figure 20: EMF as a function of log P_{O_2} [atm] for the sodium β-alumina electrolyte with air as a reference; △) 1075°K, P_{AsH_3} = 301 ppm, f.r. 1 ml/s; ○) 1075°K, P_{AsH_3} = 502 ppm, f.r. 0.5 ml/s; □) 1075°K, P_{AsH_3} = 502 ppm, f.r. = 1 ml/s; ●) 1025°K, P_{AsH_3} = 5 ppm, f.r. 1 ml/s; ■) 1025°K, P_{AsH_3} = 9.8 ppm, f.r. 1 ml/s 97

CDT
Centre de
Développement
Technologique
École Polytechnique
de Montréal

TABLES IN APPENDIX

Page

Table A.1: Experimental data for the $AgZr_2(AsO_4)_3$ electrolyte .. 98

Table A.2: Experimental data for the $NaCaAsO_4$ electrolyte 100

Table A.3: Experimental data for the Ag β-alumina electrolyte, sensor I, EMF concentration dependence 103

Table A.4: Experimental data for the Ag β-alumina electrolyte, sensor I, EMF temperature dependence 108

Table A.5: Experimental data for the Ag β-alumina electrolyte, sensor II, EMF concentration dependence 112

Table A.6: Experimental data for the Ag β-alumina electrolyte, sensor II, EMF temperature dependence 113

Table A.7: Experimental data for the Ag β-alumina electrolyte, sensor II-2, EMF temperature dependence 114

Table A.8: Experimental data for the Na β-alumina electrolyte .. 115

CDT
Centre de
Développement
Technologique
École Polytechnique
de Montréal

1. SUMMARY

An investigation has been conducted into the development of a simple potentiometric device based on a solid electrolyte which would permit one to monitor the concentrations of arsenic oxides in a gas phase at elevated temperatures (600 ~ 900°C).

The operation of the sensor is based on the potential difference at the surfaces of a solid electrolyte membrane separating a reference and a working electrode. The electrolyte is a conductor of monovalent cations. At the surface of the working electrode, the potential (i.e. the activity of the conducting cation) is defined by the equilibrium between a solid arsenate at the membrane and the concentrations of arsenic oxide and of oxygen in the gas phase. The reference electrode potential can be set by any suitable chemical system which defines the activity of the conducting cation.

Several sodium and silver conducting solid electrolytes have been identified as suitable membranes for the galvanic cell and their behavior has been tested under various conditions of temperature and concentrations of arsenic oxides.

The EMF values of the following galvanic cells

$Ag/AgZr_2(AsO_4)_3/P_{AsH_3}, P_{O_2}, Pt$ I

$Ag/Ag\text{-}\beta\text{-alumina}/P_{AsH_3}, P_{O_2}, Pt$ II

$Ag/Ag\text{-}\beta\text{-alumina}/\tilde{P}_{As_4O_6}, P_{O_2}, Pt$ III

$Pt, P_{O_2}, \tilde{P}_{As_4O_6}/NaCaAsO_4/P_{AsH_3}, P_{O_2}, Pt$ IV

$$Pt,\ P_{O_2}/Na\text{-}\beta\text{-alumina}/P_{AsH_3},\ P_{O_2},\ Pt \qquad V$$

have been measured over a wide range of temperatures, P_{AsH_3} and P_{O_2} concentrations.

The results indicate that among the several existing arsenic oxides (produced by the oxidation of arsenic), the active species controlling the activity of Ag^+ or Na^+ at the working electrode is arsenic pentoxide, As_2O_5. It is necessary to promote the equilibrium concentration of this oxide by a catalyst such as platinum. Depending on the temperature (and the activity of the cation), the arsenic pentoxide can form meta-, pyro- or orthoarsenates on the membrane. The formation equilibria of the particular arsenate stable at a given experimental condition determine the EMF dependence on P_{AsH_3} ($P_{As_2O_5}$). For both silver- and sodium-conducting electrolytes, the temperature and range of arsenic oxide partial pressures (at a constant P_{O_2}) can be found for which the EMF is a linear function of the arsenic oxide concentration.

The formation of silver orthoarsenate on the surfaces of the Ag-electrolytes has been verified by X-ray diffraction analysis and the thermal stability of the silver orthoarsenate has also been evaluated.

Both silver and sodium orthoarsenates are more stable than the corresponding sulphates and therefore a certain degree of AsO_x selectivity over SO_3 can be expected, this being higher in the case of a sodium based sensor.

While the silver-conducting electrolytes ($AgZr_2(AsO_4)_3$ and

Ag-β-alumina) are very suitable materials for the arsenic oxide sensor, they can not be used for the determination of the thermodynamics of other arsenates such as Cu, Fe or Ni since the latter are expected to be more stable than silver orthoarsenate. For these particular systems, sodium conducting electrolytes such as Na β-alumina and NASICON would be suitable.

2. BACKGROUND

Arsenic, a highly toxic element, occurs naturally in concentrations up to 15% in many Cu, Ni, Au, Ag and Fe sulphide based ores, primarily as arsenides. During pyrometallurgical processing, arsenides can be volatilized as oxides or sulphides, depending on the oxygen content in the atmosphere.

The development of effective processes for the removal of arsenic, both from the ores and the flue gases, requires reliable thermodynamic data for various metal arsenides and arsenates as well as a simple arsenic sensor.

For most metal sulphides and sulphates, the thermodynamic data are very well established, but for arsenic-bearing compounds the thermodynamic data are lacking. In addition, a simple analytical device for monitoring gaseous arsenic oxides, such as a potentiometric solid sensor developed for sulphur oxides, does not exist.

In comparison with sulphur-containing compounds, the lack of thermodynamic data for arsenic-bearing compounds is due to several factors:

- Sulphides and sulphates are often considered a valuable mineral whereas As-bearing species have always been treated as undesirable and unimportant.

- Thermodynamic properties of metal sulphides can be measured by equilibrating the metal with appropriate H_2/H_2S gas mixtures. Although H_2S is a poisonous gas, the "bad egg" odour readily alerts the research worker to potential problems before the gas

concentration reaches toxic levels (50 ppm). In principle, metal arsenides can be equilibrated with H_2/AsH_3 mixtures. However, AsH_3 (arsine) is extremely toxic. It is lethal at concentrations (1 ppm) at which the odour detection is not reliable. In addition, AsH_3 is relatively unstable and decomposes at temperatures above 300°C.

- Thermodynamic data for metal sulphates are generally obtained from decomposition pressure measurements, or from gas equilibration techniques using $SO_2(g)$. Thermodynamic data for the S-O gas species are well established. By comparison, gaseous dissociation products containing a polymorphic mixture of As and O compounds are more complex. The necessary thermodynamic data to calculate the gas phase compositions are not as reliable. Also, gas equilibration techniques involving $As_4O_6(g)$ are difficult since this compound is volatile only at elevated temperatures. The vapour pressure of arsenolite, $As_2O_3(s)$, is $\tilde{P}_{As_4O_6} \approx 10^{-3}$ atm at approximately 200°C.

In our laboratories we have employed potassium sulphate and potassium carbonate as solid electrolytes to monitor sulphur dioxide and carbon dioxide concentrations respectively and to measure thermodynamic properties of oxide-sulphate and oxide-carbonate equilibria. The same solid state device has also been used to measure the sulphur content of gases and solid materials.

Our investigation of potassium sulphate and potassium carbonate sensors has led us to the present investigation into the development of arsenic (oxide) sensors based upon similar principles.

3. OBJECTIVE

The objective of this contract was to develop a potentiometric solid state electrolyte sensor which could be used to determine at elevated temperatures the content of arsenic oxides in a gas phase containing oxygen.

4. ANALYSIS OF THE PROBLEM

The proposal for the development of a solid-state sensor for arsenic oxides was based on technology developed in this laboratory for carbon dioxide and sulfur dioxide sensors (4-11).

The operation of these sensors can be illustrated by the following reaction which takes place at the working electrode (on the surface of the solid electrolyte membrane) through which the activity of the conducting ion is controlled:

$$nM^+ + \frac{1}{i} B_iO_j + (\frac{mi - j}{2i})O_2 + ne^- = M_nBO_m \qquad [4.1]$$

M^+ is the alkali metal or silver cation, B_iO_j is the gaseous oxide and M_nBO_m is the corresponding oxysalt. If the activity of M^+ is maintained constant at the reference electrode, the EMF of the resulting galvanic cell:

$$\text{reference electrode} \,|\, \text{M^+ conducting solid electrolyte} \,|\, (O_2), (B_iO_j), \text{Pt} \qquad [4.2]$$

can be written as:

$$EMF = \text{const} + \frac{2.3RT}{nF} \log P_{B_iO_j}^{1/i} + \frac{2.3RT}{nF} \log P_{O_2}^{(mi - j)/2i} \qquad [4.3]$$

Clearly the cell can function as a B_iO_j sensor provided that the oxygen concentration P_{O_2} is known.

The successful development of a particular B_iO_j sensor and the range of its application depend on the following factors:

1) thermodynamic stability of the gaseous oxide(s), (B_iO_j),

2) physical characteristics and the thermal stability of the electrolyte,

3) reference electrode,

4) design,

5) selectivity with respect to other species.

In the case of sulphur oxides, the electrode reaction [4.1] has been shown (6) to be:

$$2M^+ + SO_3(g) + O^{2-} = M_2SO_4(s) \qquad [4.4]$$

where the sulphur trioxide (SO_3) is the active species, although for practical reasons, reaction [4.4] is usually expressed in terms of sulphur dioxide and oxygen.

Potassium and potassium-silver sulphate solutions (6), sodium sulphate (12,13), two phase lithium-silver sulphate compositions (14-16) and sodium conducting ceramic materials such as NASICON (17) and β-alumina (18,19) have been employed as SO_2 sensors. Three different reference electrodes have been proposed: solid metal, i.e. silver (6,14-16) or a gold/gold-sodium alloy system (19); circulating gas electrode (12,13,17); and a stationary gas electrode, where the SO_3 concentration is fixed by a metal sulphate in air decomposition (20). The technology acquired in the development of the SO_2 sensors has been applied to the present project for the development of the arsenic oxide sensor.

4.1 Arsenic oxides

Arsenic is known to form two stable solid oxides: arsenic trioxide, As_2O_3, and a hydroscopic arsenic pentoxide, As_2O_5 (2,21). While the arsenic pentoxide is thermodynamically more stable, under normal conditions (low temperatures and $P_{O_2} < 1$ atm) arsenic trioxide existing in two allotropes, claudetite and the more stable arsenolite, is not readily oxidized.

Arsenic trioxide is quite volatile, vaporizing as a dimer, $As_4O_6(g)$. Gaseous As_4O_6 has so far been considered as stable up to 800°C. Recent mass spectrometric studies of the unsaturated vapor over arsenolite has confirmed the existence of As_4O_6 in the vapor, but at 1050°K small amounts of AsO, As_3O_4 and As_2O_3 species have also been detected (22).

Thermodynamic properties of both forms of solid arsenic trioxide seem to be well known. The vapor pressure has been measured up to the melting point (275°C) by several workers. The most reliable data seem to be those by Behrens and Rosenblatt (23) who measured the arsenolite vapor pressure at temperatures between 95 - 151°C (23) and proposed the following equation:

$$\log \tilde{P}_{As_4O_6} = - (6067 \pm 125)\ T^{-1} + (9.905 \pm 0.319)\ (atm) \qquad [4.5]$$

Behrens and Rosenblatt have shown (23) that this equation, confirmed later by Murray, Pottie and Pupp (24), represents also very well the earlier available data for temperatures up to 550°K.

Skeaff and coworkers (25) used arsenolite at various temperatures (150 - 220°C) as a source of an As_4O_6 vapor in their thermodynamic measurements of equilibrium constants of several reactions of the type:

$$Ni_mAs_n + \frac{2m + 3n}{4} O_2 = mNiO + \frac{n}{4} As_4O_6 \qquad [4.6]$$

Arsenic pentoxide is much less volatile and until recently was considered to decompose at temperatures above 450°C to oxygen and As_4O_6:

$$As_2O_5(s) = \tfrac{1}{2} As_4O_6(g) + O_2(g) \qquad [4.7]$$

Based on this assumption, the equilibrium constant for reaction [4.7] was measured at 558 and 593°C by Guérin and Boulitrop (26) and later by Polukarov, Makhmetov and Buketov (27) at temperatures between 550 and 730°C.

However, Von Plies and Jansen (28) have shown by mass spectrometry, that at temperatures between 862 - 939°K, the vapor over the solid As_2O_5 is composed of the following species: O_2, As_4O_6, As_4O_7, As_4O_8, and much smaller proportions of As_4O_9 and As_4O_{10}. Barten and Cordfunke (29) studied the arsenic pentoxide vaporisation at temperatures between 865° and 1009°K by using the transportation method to analyze the vapor composition and a static method to determine the oxygen pressure over the sample. By chemical analysis, they found that the vapor condensate contained both the trioxide and the pentoxide (30-50%) and that the arsenic oxide pressure was independant of oxygen. This led them to the conclusion that the arsenic pentoxide dissociation takes place in the vapour phase and that it is slow compared with to rate of vaporization..

No other information has been found on the oxidation of gaseous arsenic trioxide.

In the light of these articles, it can be concluded that under appropriate conditions, arsenic trioxide should contain an equilibrium concentration of pentoxide, the two concentrations being related by the equilibrium constant for the reaction:

$$As_4O_6(g) + 2O_2(g) = As_4O_{10}(g) \qquad [4.8]$$

To define the total arsenic oxide concentration, the two following gas trains were evaluated:

a) arsenolite, $As_2O_3(s)$, heated in a reservoir to a known temperature which would define the vapour pressure. A carrier gas (air or nitrogen) passed over the heated arsenolite would contain a defined amount of As_4O_6 which could be calculated from equation [4.5] and the known temperature of the arsenolite reservoir. Oxygen can then be added to the gas in order to increase the partial pressure of O_2 and dilute the As_4O_6 concentration.

b) arsine mixed with oxygen which would then be completely oxidized at high temperatures. In our case this was experimentally more attractive. The use of arsine permits a simpler design of the sensor and provides a convenient means of changing the gas composition.

Arsine, AsH_3, is a highly toxic thermodynamically unstable gas. Even at room temperatures, the equilibrium dissociation constant is relatively high and at 300°C arsine should be completely decomposed. However, since the rate of the decomposition up to 400°C is negligibly small (30), it can take several hours to achieve complete dissociation.

The available kinetic data (30) indicates that only above 650°C can 99% decomposition be attained within a second.

On the other hand, the oxidation of gaseous arsenic is rapid even at temperatures as low as 80°C (31-32) and apparently takes place via the metastable AsO_2 and AsO molecules which combine to form a stable trioxide and possibly pentoxide.

Thus, it is reasonable to assume, that at sufficiently high temperatures, arsine oxidation is complete even at relatively low oxygen concentrations provided that the initial oxygen concentration is greater than the arsine concentration. Therefore, the concentration of arsenic oxide(s) can be defined by a concentration of arsine, provided that the small amount of water resulting from arsine oxidation can be considered as inert.

Having defined the total concentration of arsenic oxide(s) $P^t_{As_4O_x}$, by means of either an arsenolite reservoir or an AsH_3/air (or AsH_3/oxygen) mixture and assuming only As_4O_6 and As_4O_{10} molecules are formed, we can express the equilibrium concentration of As_4O_{10} as:

$$P_{As_4O_{10}} = P^t_{As_4O_x} \left(\frac{K_{ox} P^2_{O_2}}{1 + K_{ox} P^2_{O_2}} \right) \qquad [4.9]$$

where K_{ox} is the equilibrium constant of reaction [4.8]. Although the value of K_{ox} is unknown (the available data suggests a low value) it should be possible to estimate it from the experimental results.

4.2 Solid electrolytes

For gas sensors in general, the material used as the solid electrolyte membrane should have very good mechanical and chemical stability, a sufficiently high ionic conductivity, and a low gas permeability. In addition, to operate as an arsenic oxide sensor, the electrolyte should be an arsenate salt or a material on which an insoluble (in the support electrolyte) layer of an arsenate can be formed in situ. In this respect, several solid electrolytes can be identified as potentially suitable. These are listed in Table 1 along with some of their characteristics. Ionic conductivity values of the listed materials are not available. However, by analogy with other alkali salts of the type A_nBX_m (33), they can be expected to be reasonably high. The ionic conductivities of the ceramic-type electrolytes are known to be high even at temperatures as low as 300°C (34-36).

Based on the earlier work on SO_2 and CO_2 sensors (6,9-11,8), potassium orthoarsenate was initially considered as a good candidate. However, it was found to be extremely hygroscopic and it was excluded from further work since it would not offer any special advantage over sodium arsenate. Apart from the expected higher ionic conductivity, lithium arsenate also does not appear to offer any advantages over sodium arsenate. In fact, sodium arsenate is the least hygroscopic among these three alkali metal arsenates. In addition, an interest in sodium arsenate as potential electrolyte stems from the fact that its formation would be expected on the surface of any other electrolyte conducting exclusively sodium ions, such as $NaCaAsO_4$, Na β-alumina and NASICON. While sodium calcium arsenate exhibits polymorphism up to 765°C, it is less hydroscopic and the pellets have a better mechanical stability than those of sodium arsenate.

TABLE 1

SOLID ELECTROLYTES POTENTIALLY SUITABLE AS ARSENIC OXIDE SENSORS

	ELECTROLYTE	POLYMORPHISM	CRYSTAL STRUCTURE	m.p. °C	MECHANICAL STABILITY	CHEMICAL AND THERMAL STAB.
1	Li_3AsO_4	~680°C	(37)	1150	--	m.a.; p.a. hygroscopic
2	K_3AsO_4	not known	--	1250	good	m.a.; p.a. ext. hygroscopic
3	Na_3AsO_4	250°C, 410°C	(37)	1260	good	m.a.; p.a. hygroscopic
4	$NaCaAsO_4$	285°C, 485°C, 765°C	(39,40)	>1200	very good	less hygroscopic
5	$NaZr_2(AsO_4)_3$	no	(36,41)	>1200	excellent	
6	Na β-alumina	no	(34)	~1600	excellent	
7	$AgZr_2(AsO_4)_3$	no	--	> 990	very good	
8	Ag β-alumina	no	(35)		excellent	
9	NASICON (arsenate based)	no	(36)		excellent	

m.a.: metaarsenate; p.a.: pyroarsenate.

The main advantages in the application of the ceramic electrolytes as gas sensors are their excellent mechanical stability, negligible gas permeability, and the possibility of casting the electrolyte in a variety of shapes, an important factor to be considered when designing a sensor for an industrial applications.

Both NASICON, $Na_3Zr_2Si_2PO_{12}$ (17), and Na β-alumina (19) have been shown to function very well as SO_2 sensors, although the response time was longer in both cases than in the case for potassium sulphate (6). These materials should prove equally suitable as arsenic oxide sensors. However, when the NASICON family is considered, arsenate-based compounds should be preferable not only for improved ionic conductivity (36) but also for the expected better compatibility with the arsenate formed on the surface.

With respect to the choice of the reference electrode (next section) silver-conducting electrolytes are attractive due to the possibility of using silver metal as the reference electrode.

Although silver arsenate could form on the surface on any silver conducting electrolyte, it would not be suitable by itself since its electronic conductivity is relatively high (42).

Having for practical reasons limited the electrolytes to sodium and silver conductors, we found it of interest to examine further the stability of sodium and silver arsenates. With sodium or silver, arsenic oxide forms several arsenate compounds (21,43,45,47). Ultimately the formation of a given compound on the surface of the electrolyte would dictate the response of the sensor to the arsenic oxide concentration. Table 2 presents the available data. No reliable thermodynamic data based on the thermal decomposition of any of the compounds in Table 2 are available. Nevertheless, in the case of

TABLE 2

PROPERTIES OF SILVER AND SODIUM ARSENATES

$M_2O:Ag_2O_5$	COMPOUND	m.p. °C	STABILITY	REF.
1:1	$AgAsO_3$	~440	dec. > 250°C	43,45
			↓	
2:1	$Ag_4As_2O_7$	~520	dec. > 600°C	43,45
			↓	
3:1	Ag_3AsO_4	~830	dec. ~ 800°C	43
		810-830	dec. > 870°C	45*
		770-870	dec. > 1100°C	44*
1:1	$NaAsO_3$	615	615°C	46,47
			↓	
5:3	$Na_5As_3O_{10}$	680	680°C	46,47
			↓	
2:1	$Na_4As_2O_7$	845	845°C	46,47
3:1	Na_3AsO_4	1260	dec. 1300°C	46,47

* Both references present X-ray diffraction spectra and DTA thermograms, a phase change at ~665°C was observed on the thermograms.

silver arsenate, the data seem to be sufficient to assume that at temperatures above 600°C, the pyroarsenate would form only in the presence of a very high arsenic pentoxide concentration. Thus, the working range with a single linear relationship between EMF and the arsenic oxide vapor pressure should be situated between 670 and 850°C. This temperature range is inside the range of interest of pyrometallurgical roasting operations.

The formation of pyroarsenate would be expected in the case of sodium conductors. This by itself might not necessarily be a limiting factor in a given application, as long as a temperature region can be found for which the EMF of the sensor and the gaseous concentration of arsenic oxides are related by a simple function.

4.3 Reference electrodes

The available reference electrode systems can be divided into three groups according to their physical state:

a) solid reference

b) liquid reference

c) gaseous reference

The choice of the appropriate reference system is dictated by the thermodynamic stability of the electrolyte membrane and by the practical aspects of its particular application.

For practical reasons, the liquid reference systems were not considered in this investigation. In industrial applications, solid state reference systems are the most convenient.

With silver-conducting solid electrolytes, silver metal is particularly attractive and leads to a simple and convenient design. Although gaseous reference systems can be employed and in some special applications are more suitable, they were not included.

On the other hand, with sodium conducting electrolytes, solid state reference systems are not readily available. The gold/gold-sodium alloy system proposed by Kozuka (19) is rather costly, requires an inert atmosphere and an independent determination of the sodium activity. The powder system of W, WS_2 and Na_2S first used by Liang and Elliott (48) and later successfully employed by Dubreuil, Malenfant and Pelton (49) in the measurements of Na β-alumina stability, would not be practical since it also requires an oxygen-free atmosphere. For sodium-conducting electrolytes it was therefore necessary to consider gaseous references. As shown by Gauthier and coworkers (20), these could be either:

a) a stationary gas system in which the composition of the gas fixing the metal activity at the electrode is defined by the decomposition of a suitable oxysalt in atmospheric oxygen diffusing into the electrode compartment (10).

or b) a circulating gas of a known composition. For Na β-alumina in principle (19, 49) this could be pure air.

Both gaseous reference systems were considered appropriate in this investigation. In fact, both gas references or a combination of the stationary gas electrode with some other reliable reference, offered a means of determination of the thermal stability constant of the salt used in the system.

As a circulating gas system, an arsenolite (As_2O_3) reservoir

was chosen as a convenient alternative to arsine, although both arsenic oxide sources (As_2O_3 or AsH_3) were potentially suitable.

4.4 Design of the sensor

In general, the solid electrolyte potentiometric cell consists of two gas-tight electrodes, separated by an electrolyte membrane. The membrane is usually in the form of a disc-pellet or a closed-end tube (50). Each form offers some special advantage.

The pellet design, such as that proposed by Gauthier and coworkers (4,6,10), is especially suitable for exploratory work with materials which can not be cast or for which the casting technique is not well established. A modification of this design used earlier for SO_2 and CO_2 sensors (7-9,11) is shown in Figure 1. This design is particularly suitable for materials exhibiting a certain degree of ductility which permits a gas-tight separation of the compartments simply by compression of the gas-compartment tube against the pellet. With ceramic electrolytes it may be difficult to achieve the required gaseous impermeability.

The design shown in Figure 1 is also suitable for thermodynamic measurements.

For industrial applications, a design based on the closed-end tube is preferable. Two variants of such a design are shown in Figure 2a and 2b. These were employed for the Na β-alumina and Ag β-alumina studies.

4.5 Selectivity and Range of Application

Selectivity, concentration sensitivity, and temperature response-sensitivity are the decisive factors in the applicability of any sensor to a given problem. It is easy to see that each particular application places its own special requirements on the probe.

With respect to the objective of this project, the two expected applications:

a) an industrial sensor for monitoring the gaseous arsenic oxides concentrations in pyrometallurgical processes,

and b) a galvanic cell for measuring the thermodynamic properties of base metal arsenates;

place quite different requirements on the sensor.

4.5.1 An arsenic oxide sensor for pyrometallurgical processes:

In roasting operations, the typical operating temperatures are between 500 - 900°C, with the optimum in the range of 600 - 800°C. Since arsenic is commonly an impurity in the sulphide-based ores, a large excess of sulphur dioxide over arsenic oxides (> 100 fold) would be expected in the flue gases. Sulphur oxides are the major potential interference, although the presence of Se, Sb and Bi impurities might also affect the selectivity of the cell.

Unless a simple process to eliminate SO_2 selectively before the analysis for arsenic oxides can be found, the sensor in question must be highly selective with respect to arsenic. In addition it must function reliably at temperatures between 600 - 800°C and be of a simple design.

The previous analysis suggests that the latter two requirements might best be met by the use of a silver conducting electrolyte in a design similar to that of Figure 2b.

The selectivity of this type of sensor is expected to depend upon the thermal stability of the compound being formed on the electrolyte. Due to the relatively high thermal stability of the sodium and silver sulphates, a very good selectivity for SO_2 gas in the presence of CO_2 has been shown experimentally for silver sulphate-based sensors (16) and NASICON based sensors (17) as well as by calculations in the case of Na β-alumina (51).

Although we do not have the necessary data for silver arsenate to perform the calculations similar to those in reference (51), a qualitative estimate can be made based on published experimental results (43, 45). In Table 3, the known thermal properties of silver sulphate and silver arsenate are compared.

TABLE 3

THERMAL PROPERTIES OF Ag_2SO_4 and Ag_3AsO_4

	m.p.	decomp. by thermal analysis	ref.
Ag_2SO_4	652°C	> 800°C	(52)
Ag_3AsO_4	≈ 800°C	> 870°C > 1100°C	(45) (44)

Using these data as a guideline, a preferred selectivity of the silver-based sensor to arsenic oxide over sulphur oxides would be expected.

4.5.2 Galvanic cell for the determination of the thermodynamic properties of several base-metal (Cu, Co, Ni, Fe) arsenates:

Silver salts are generally less stable than corresponding Cu, Co, Ni, Fe, etc. salts. Thus, silver-conducting electrolytes would not be suitable for the determination of their thermal stability. Rather, a sodium-conducting electrolyte should be employed.

With respect to the design, the apparatus shown in Figure 1 is very appropriate for performing thermodynamic measurements.

5. EXPERIMENTAL

5.1 Gases

With arsine as a source of arsenic oxide(s), a mixing system (in Figure 3) was designed, assembled and tested for leaks at a pressure of 30 psi. The gas train consisted of 1/8" 316 stainless steel tubing, three ball flowmeters, three fine metering valves, two U mercury filled manometers, three shut off valves, two mixing chambers all connected by 316SS SWAGELOCK fittings. The flowmeters were calibrated at 26 psi and 25°C (the ambient temperature) with the aid of a soap bubble flowmeter. The calibration was periodically verified, particularly when the ambient temperature changed by more than 2°C. In this manner it was possible to keep the error in flowrate to within 3%.

Desired arsine and oxygen concentrations were prepared by mixing appropriate ratios of arsine (98 or 5020 ppm) diluted in nitrogen, oxygen and nitrogen, or air. High purity, extra dry gases (nitrogen, oxygen, air) were used without further purification. The diluted arsine was analysed by the supplier (Union Carbide) and the concentrations reported to be accurate to within 1%.

When arsenolite was used as a source of arsenic oxide, the saturated vapor was produced by passing a carrier gas over arsenolite held in a stainless steel container heated by oil at temperatures up to 150°C ± 0.1°C, maintained by a HAAKE E52 temperature control unit. The saturator is shown in Figure 4. The temperature at the outlet of the saturated gas was monitored by a K-type thermocouple connected to a Keithley 871 digital thermometer. The gas line connecting the saturator and the probe was heated by means of a heating tape maintained at least 10°C higher than the saturator. The nitrogen (or air) used as a carrier gas was preheated before entering the saturator

by passing it through a copper tube (1/8" diam.) coiled around the saturator.

At the outlet of the galvanic cell, the arsenic oxides were scrubbed from the carrier gas by a sodium hydroxide solution.

Except for the initial experiments with $AgZr_2(AsO_4)_3$ electrolyte, flowrates in the range of 0.15 ml/s - 1.4 ml/s were used throughout this project. Higher flowrates (up to 4 ml/s) rapidly blocked the outlet of the gas electrode and were also unfavorable to the kinetics of arsine oxidation.

5.2 Solid Electrolytes

The electrolytes in Table 1 were prepared in the laboratory by high temperature powder synthesis except for Na β-alumina which is commercially available. The details of each synthesis are presented in Table 4.

Stoichiometric amounts of the initial compounds were well-ground in a motar, then carefully weighed, thoroughly mixed and finally heated to the temperatures shown in Table 4. The weight loss due to heating was used as indicator of the synthesis advancement. When the theoretical weight loss was obtained, the synthesis was considered as complete. The material was then ground in a motar and analysed by X-ray diffraction with CuK_α radiation. The resulting spectra are represented in Figure 5.

The solid electrolyte pellets, 0.1 cm thick and 0.62 cm diameter, were prepared by compressing 0.1 - 0.3 g of finely ground compound at a pressure of about 10 T cm^{-2} applied for 2 min. The pellets were sintered at the temperatures indicated in Table 4.

TABLE 4

CONDITIONS FOR THE SYNTHESIS OF SOLID ELECTROLYTES

ELECTROLYTE	INITIAL COMPOUNDS	INITIAL WEIGHT g	YEILD g	HEATING °C hr	SINTERING °C hr
Na_3AsO_4	$Na_2HAsO_4 \cdot 7H_2O$	14.1		180 16 600 10	500 6 then steps of
	Na_2CO_3	2.39	9.38 100.65%	and finally 890 12	100 1 of 1100 12
$NaCaAsO_4$	Na_2CO_3	2.12		180 ≃18 600 18	500 6 then steps of
	$CaCO_3$	4.005	9.020	and finally	100 1
	$As_2O_5 \cdot xH_2O$[a]	5.948	99.50%	1200 12	to 1200 16
$NaZr_2(AsO_4)_3$	Na_2CO_3	0.53		190 ≃18 560 20	500 6 then steps of
	$Zr(SO_4)_2 \cdot 4H_2O$[b]	7.108	6.08	and finally	100 1
	$As_2O_5 \cdot H_2O$[a]	4.312	98.9%	890	of 1200 16
$AgZr_2(AsO_4)_3$	$AgNO_3$	1.698		180 ≃18 560 12	then steps of
	$Zr(SO_4)_2 \cdot 4H_2O$[b]	7.108	6.84	and finally	100 2
	$As_2O_5 \cdot H_2O$[a]	4.312	99.2%	750 18	of 940 12

m.a.: metaarsenate ; p.a.: pyroarsenate.
a - 19.9% water by chemical analysis
b - 35.1% ZrO_2 by drying and calcination

Sodium β-alumina closed-end round-bottom tubes, 3 cm long, 0.95 cm and 0.63 cm outside and inside diameter respectively, were supplied by POLYCERAM Inc.

Silver β-alumina tubes of the same dimensions as above were prepared by an ion-exchange method consisting of soaking the tubes in molten silver nitrate at 255°C for 72 hr.

Silver orthoarsenate, for use as a reference, was prepared by precipitation of ammonium arsenate by silver nitrate from an aqueous solution with pH ≃ 4. The dark brown precipitate was washed with distilled water and dried overnight at 150°C. The resulting compound was calcinated at 690°C overnight and then for an additional 6 hr at 720°C in air, thus causing a weight loss of only 0.4%. The X-ray diffraction pattern of the calcined Ag_3AsO_4 agreed with that published by Gorokhova and coworkers (45).

5.3 Cell Assembly

The galvanic cell assembly illustrated in Figure 1 was employed for the experiments carried out on sodium calcium arsenate and silver zirconium arsenate.

All three electrodes were used in the case of sodium calcium arsenate. For the stationary gas reference, a homogeneous powder mixture of silver orthoarsenate and silver metal was placed in the small alumina crucible (right side of the electrolyte pellet).

A similar assembly was used for the experiments with silver zirconium arsenate. The reaction mixture crucible was left empty and

the platinum electrode wound on the Al_2O_3 ring contacting the electrolyte was replaced by a silver disc (0.025 cm) and a silver wire was used as an electrical lead. In addition, the thermocouple was placed on the exterior of the insulating alumina tube with the tip at the level of the electrolyte pellet.

For the sodium and silver β-alumina electrolyte tubes, the galvanic cells were constructed in a one-piece, compact form shown schematically in Figure 2. This type of probe consisted of an electrolyte tube sealed to a 4 bore alumina tube, 0.625 cm in diameter and approximately 40 cm long. COTRONIX 940 fast cure ceramic adhesive was used as a sealant. The bottom portion of the electrolyte tube surface was platinized by means of a solution of hexachloroplatinic acid.

In the case of sodium β-alumina, both sides of the electrolyte were platinized and lined with platinum mesh held in contact with platinum wire electrodes. The Pt/Pt-10%Rh thermocouples were placed in the contact with inner surface which served as a reference (Figure 2a) when equilibrated with a constant flow of air (0.5 ml s^{-1}). The assembled probe was positioned in a closed alumina tube (60 cm long and 3.1 cm in diameter) with openings for entrance and exit of the gas mixtures as shown in Figure 2c. This design eliminated the problem of blockage of the outlet tubes.

In the case of silver β-alumina, only the side on the working electrode was platinized. In the first design (Figure 2a), the outside surface was wrapped by a silver wire which served as the reference. In the second design, the reference (silver metal) was placed on the inner side. To assure a good contact, the bottom of the tube was partially filled with silver metal powder and the silver wire passed through the alumina tube left open to the exterior. The complete experimental

assembly for this probe was similar to that for sodium β-alumina (Figure 2c).

In all cases the exterior alumina tube, in close contact with the heating elements, was wrapped in a grounded stainless steel screen in order to shield the cell against AC field effects.

5.4 Temperature control

The assembled galvanic cells were heated in a Lindberg Hevy Duty horizontal furnace whose temperature was controlled to within 1°C by a Hewlett - Packard 240 temperature Programmer.

5.5 Temperature and E.M.F. Measurement

Temperatures of the galvanic cells were measured with type S (Pt/Pt-10%Rh) thermocouples, read to within 1°C with a calibrated Doric Trendicator 402 digital thermocouple meter.

EMF values were measured to within 0.1 mV by a TACCUSSEL Aries 20000 millivoltmeter (impedance $10^{12}\ \Omega$) or a Keithley high impedance ($10^{14}\ \Omega$) 614 Electrometer. Both the temperature and the EMF values were recorded with a SOLTEC 1242 Dual pen recorder.

When an experimental run was completed, the cell was dissassembled and the surface of the electrolyte analysed by an X-ray diffraction method.

6. RESULTS AND DISCUSSION

Among the prepared electrolytes listed in Table 4, silver zirconium arsenate is a new compound. Its properties and method of preparation have not been published before, although the structure and ionic conductivity of its sodium homolog (36) have been determined and the ionic conductivity and thermal expansion of several double arsenates of thorium and monovalent metals (M^+ = Li, Na, K, Ag and Tl) have been reported (53, 54). The zirconium arsenates (36) were preferred in this project since they exhibit apparently higher ionic conductivities than the thorium arsenates (55) and the zirconium salts for their synthesis are readily available.

The new direct method of preparation of this silver conducting electrolyte proved efficient and reliable, and resulted in a highly sinterable material.

Unfortunately, the scope of this project did not permit a detailed characterisation of physical properties of any of the electrolytes including the new promising material, $AgZr_2(AsO_4)_3$.

The selected electrolytes were mainly evaluated with respect to their response to temperatures and to various $P^t_{As_4O_x}$ and P_{O_2} concentrations.

Where necessary, corrections were made for the thermoelectric effect of the Ag - Pt couple by using a value of 6.5×10^{-6} V per 1°C (55).

6.1 Evaluation of the $AgZr_2(AsO_4)_3$ electrolyte

Only a limited number of measurements on two separate pellets of this electrolyte were carried out due to the following experimental problems:

a) difficulties in obtaining a perfect gas separation of the reference and the gas electrode,

and b) blockage of the gas outlet tubes (1/16" diameter) by condensing arsenic oxides.

Nevertheless, the results obtained were valuable in planning the other experiments. The results indicated that the development of a potentiometric arsenic sensor was indeed feasible.

Prior to the measurement of EMF values as a function of $p^t_{As_4O_x}$ concentration, an attempt was made with each pellet to evaluate the stability of the electrolyte by measuring the EMF of the cell:

$$Ag \left| AgZr_2As_3O_{12} \right| P_{O_2}\ (air);\ P_{AsH_3} = nil,\ Pt \qquad [6.1.1]$$

at temperatures between 350 and 800°C. Fairly stable values of EMF were obtained, in agreement within 50 mV for the two pellets. It was observed that between 400 and 550°C, the EMF values increased with increasing temperature but at temperatures higher than 550°C the EMF decreased. The temperature dependence could approximately be expressed as:

$$EMF \simeq (85 + 0.2\ T)\ mV\ (673°K < T < 823°K) \qquad [6.1.2]$$

$$EMF \simeq (720 - 0.55\ T)\ mV\ (823°K < T < 1073°K) \qquad [6.1.3]$$

CDT
Centre de
Développement
Technologique
École Polytechnique
de Montréal

In order to measure the EMF values of the galvanic cell:

$$Ag \left| AgZr_2As_3O_{12} \right| P_{AsH_3}, P_{O_2}, Pt \qquad [6.1.4]$$

as a function of P_{AsH_3} and P_{O_2} (at a constant temperature), the cell was first allowed to equilibrate with P_{O_2} = 0.21 atm and P_{AsH_3} corresponding approximately to the middle of the range of concentrations utilised. Both pellets responded immediately when arsine was introduced. The EMF value first decreased, but within seconds started to increase. It took about 2 hr to obtain values stable to within 1 mV for a period of at least 30 min. After the initial equilibration period, the time to obtain a steady EMF value upon a change in concentration was 5-20 min. and depended on the magnitude of the change in concentration.

With the first pellet, only a few results were obtained since the electrical contact of the Ag - electrode became accidently broken. At 711°C, P_{O_2} = 0.21 atm and P_{AsH_3} = 79 ppm, an EMF ≈ 425 mV was obtained after 3 hr. A dark brown deposit (Ag_3AsO_4) formed on the surface of the pellet.

With the second $AgZr_2(AsO_4)_3$ pellet, the EMF was measured at 613°C as a function of P_{AsH_3} and P_{O_2}. The temperature was kept constant to within 1°C. In experiments lasting four days, the following ranges of P_{AsH_3}, P_{O_2} and total flowrates were employed: 1.3 ppm < P_{AsH_3} < 1200 ppm; 0.15 atm < P_{O_2} < 0.98 atm; 0.8 ml/s < flowrate < 4 ml/s. The range of flowrates corresponded to values used for SO_2 sensors (6-18,21). On any one day, reproducible EMF values were obtained, but for some concentrations a shift up to 30 mV in EMF values was observed compared to the data from different days. Nevertheless,

the EMF always increased with increasing P_{AsH_3} and or P_{O_2}, but only up to P_{AsH_3} ≈ 250 ppm (P_{O_2} ≈ 0.95 atm). For higher values of P_{AsH_3}, the EMF unexpectedly decreased. As will be discussed later, an upper P_{AsH_3} limit was also found with the other electrolytes.

The upper limit increased with increasing temperature. The kinetics of the complex arsine oxidation reaction appears to be the source of this effect.

Except at high P_{AsH_3}/P_{O_2} ratios, the effect of the flowrate was within 10 mV.

After four days of operation, the back pressure at the gas electrode rapidly increased, apparently due to blockage of the exit tubing, and the values of EMF started to drift. Consequently, the experiments were terminated with a heating test. At a flowrate of 0.85 ml/s, and a gas mixture of P_{AsH_3} = 18.5 ppm and P_{O_2} = 0.82 atm, the cell was heated at the rate of 0.5°C/min to 780°C. A linear decrease of EMF was observed for temperatures between 730 - 780°C, with the slope of 1.3 mV/°C. A dark brown deposit formed on the side of the gas electrode and apparently started to form also at the reference side. The deposit was subsequently identified by X-ray analysis as Ag_3AsO_4.

The following linear function relating EMF and P_{AsH_3} and P_{O_2} concentrations represented the selected set of data very well (56):

$$EMF = 701 + 59 \log P_{AsH_3} P^2_{O_2} \qquad [6.1.5]$$

All the results are presented in Figure 6. The results can be divided into 3 different sets, each having approximately the same higher than theoretical (14.6 mV) slope.

In spite of the unexpected response and their limited reliability, the results indicating a fairly good thermal stability of Ag_3AsO_4 (of the order of 50 kcal at 886°K, based on the value of the intercept in equation [6.1.5]) were considered as very encouraging. However, no attempt for interpretation was made at this time.

Due to the experimental problems encountered with this electrolyte, it was decided to evaluate the other electrolytes and to determine what were the common important factors controlling the electrode reactions. Since the pellets of sodium orthoarsenate proved to be porous possibly due to high hygroscopicity, sodium calcium arsenate was chosen as an alternative electrolyte.

6.2 Evaluation of the $NaCaAsO_4$ electrolyte

The evaluation of this electrolyte was based on measurements carried out on a single pellet of $NaCaAsO_4$ over a three week period.

In order to reduce the clogging of the gas outlets by condensing arsenic oxides, the flowrates were reduced and only the lower range of arsine concentrations was employed.

At the beginning of the experimental run, it was difficult to obtain a completely gas-tight seal at the electrodes. However, at higher temperatures by applying a higher compression to the housing, an acceptable seal was achieved.

CDT
Centre de
Développement
Technologique
École Polytechnique
de Montréal

As a further precaution against possible leaks between the electrodes, the flowrates at the two circulating gas electrodes were kept at the same value.

As in the first series of experiments ($AgZr_2(AsO_4)_3$), at the end of each working day the flow of gases was discontinued. The cell responded immediately when arsine was introduced, but it took about 1.5-2 hr to obtain steady EMF values. However, when the concentrations were changed by small amounts, steady values were obtained within 200s. On any given day, the EMF values were reproducible to within 2 mV. The overall reproducibility was better than 20 mV.

At the beginning of an experimental run, only air was passed over the two circulating gas electrodes. When EMF values lower than 15 mV were observed, the arsenolite bath was employed. The cell:

Pt, air over heated arsenolite $\left|NaCaAsO_4\right|$ air, Pt [6.2.1]

responded by a difference of approximately 100 mV when the arsenolite bath reached the selected temperature (111.3°C). No change was observed, however, in the EMF values of the other cell, i.e.:

Pt, Ag, Ag_3AsO_4, air $\left|NaCaAsO_4\right|$ air, Pt [6.2.2]

and this was taken as an indication of the reliability of the experimental set up.

No independant check on the $As_4O_6(g)$ concentration at the reference was carried out.

EMF values of following cells were then measured at 802°C, 744°C and 676°C:

$$Pt, air, \underset{(r)}{\tilde{P}_{As_4O_6}} = 1.3\ ppm \left| NaCaAsO_4 \right| P_{AsH_3}, \underset{(w')}{P_{O_2}}, Pt \qquad [6.2.3]$$

$$Pt, air, \underset{(r)}{Ag, Ag_3AsO_4} \left| NaCaAsO_4 \right| P_{AsH_3}, \underset{(w)}{P_{O_2}}, Pt \qquad [6.2.4]$$

The following reactions were expected to take place at each electrode:

$$1/2\ O_2(g) + 2e = O^{2-} \qquad [6.2.5]$$

$$6Na^+ + 3O^{2-} + 1/2As_4O_{10}(g) = 2Na_3AsO_4(s) \qquad [6.2.6]$$

and at lower temperatures possibly:

$$4Na^+ + 2O^{2-} + 1/2As_4O_{10}(g) = Na_4As_2O_7(s) \qquad [6.2.7]$$

Defining $P_{As_4O_{10}}$ as:

$$P_{As_4O_{10}} = P^t_{As_4O_x} K_{ox} P^2_{O_2} (1 + K_{ox} P^2_{O_2})^{-1} \qquad [6.2.8]$$

where K_{ox} is the equilibrium constant for the oxidation of As_4O_6,

$$As_4O_6 + 2O_2 = As_4O_{10} \qquad [6.2.9]$$

we can express the EMF values as:

$$EMF = \frac{2.3RT}{6F} \frac{1}{2} \log \frac{[P^t_{As_4O_x} K_{ox} P^2_{O_2} (1 + K_{ox} P^2_{O_2})^{-1} P^3_{O_2}]_w}{[P^t_{As_4O_x} K_{ox} P^2_{O_2} (1 + K_{ox} P^2_{O_2})^{-1} P^3_{O_2}]_r} \qquad [6.2.10]$$

or

$$EMF = \frac{2.3RT}{4F}\frac{1}{2}\log\frac{[P^t_{As_4O_x}K_{ox}P^2_{O_2}(1 + K_{ox}P^2_{O_2})^{-1}P_{O_2}]_w}{[P^t_{As_4O_x}K_{ox}P^2_{O_2}(1 + K_{ox}P^2_{O_2})^{-1}P_{O_2}]_r} \qquad [6.2.11]$$

for the case of $Na_4As_2O_7$ formation.

It is clear that, regardless of the values of $P^t_{As_4O_x}$ and P_{O_2} at the reference, for $K_{ox}P^2_{O_2} << 1$ and $(P^t_{As_4O_x})_w = 0.25\ P_{AsH_3}$ the EMF could simply be written as:

$$EMF = const + \frac{2.3RT}{12F}\log P_{AsH_3}P^5_{O_2} \qquad [6.2.12]$$

or

$$EMF = const + \frac{2.3RT}{8F}\log P_{AsH_3}P^3_{O_2} \qquad [6.2.13]$$

for the case of $Na_4As_2O_7$ formation.

In addition, for:

$$(P^t_{As_4O_x}P^5_{O_2})_r = (P^t_{As_4O_x}P^5_{O_2})_w \qquad [6.2.14]$$

or

$$(P^t_{As_4O_x}P^3_{O_2})_r = (P^t_{As_4O_x}P^3_{O_2})_w \qquad [6.2.15]$$

the EMF should be equal to zero.

The reference values of $P^t_{As_4O_x}$ and P_{O_2} were known only for the cell [6.2.3].

CDT
Centre de
Développement
Technologique
École Polytechnique
de Montréal

For the cell [6.2.4] only $(P_{O_2})_r$ was known. The values of $(P^t_{As_4O_x})_r$ and consequently that of the constant in equations [6.2.12] and [6.2.13] could not be evaluated a priori since the equilibrium constants for silver arsenate decomposition were not available. Nevertheless, the EMF values with this cell were reproducible and consistent with expectations. Table 5 lists the observed values for $EMF_{[6.2.4]} - EMF_{[6.2.3]}$.

TABLE 5

VALUES OF $EMF_{[6.2.4]} - EMF_{[6.2.3]}$

TEMPERATURE °K	$EMF_{[6.2.4]} - EMF_{[6.2.3]}$ mV
1075	41 ± 3
1017	30 ± 2
949	-80 ± 4

These measurements indicated that the Ag/Ag_3AsO_4 half-cell could in principle serve as a convenient reference. However, for the purpose of further treatment only the values of $EMF_{[6.2.4]}$ were used.

In Figure 7, the EMF values are plotted as a function of $\log P_{AsH_3} P^5_{O_2}$. The fit appears reasonably good and at 1075°K the slope of the line corresponds to the expected value, but at 943°K and 1017°K the slopes of the lines are higher than the theoretical values calculated from [6.2.12]. In addition, the value of the constant in equation [6.2.12] is too high. At $\log P_{AsH_3} P^5_{O_2} = -8.67$, corresponding to the concentration at the reference electrode, the EMF should be zero at all temperatures.

When plotting $EMF_{[6.2.4]}$ as a function of log $P_{AsH_3} P^3_{O_2}$, a better fit is obtained, but all slopes are much higher than theoretical values and also the value of the constant in equation [6.2.13] is much too large. In this case an EMF equal to zero would be expected at log $P_{AsH_3} P^3_{O_2}$ = -7.32.

In fact, regardless of the value of $K_{ox} P^2_{O_2}$, much lower EMF values would be expected whether the electrode reaction involves the formation of orthoarsenate or pyroarsenate. At 949°K, P_{AsH_3} = 77.3 ppm and P_{O_2} = 0.21 atm, the expected EMF value would be 18 mV or 28 mV respectively, but the observed value (Table A.2) is 351 mV.

The unexpectedly high values of the "const." in equation [6.2.12] and [6.2.13] and an unexpectedly high sensitivity of EMF to temperature would suggest a different reaction mechanism at the two electrodes. It is unlikely that any further mathematical analysis of the available data would help to explain the observed EMF response to variations in P_{AsH_3}, P_{O_2} and temperature.

In view of these complications it was decided to perform the subsequent experiments on silver and sodium β-alumina electrolytes. By using silver (and air) as the reference, the use of these electrolytes permitted an independant study of the EMF response to As_4O_6 - oxygen and AsH_3 - oxygen mixtures.

6.3 Evaluation of the Silver β-Alumina Solid Electrolyte

The objective of this evaluation was not only to analyse the suitability of silver β-alumina as an arsenic oxide sensor, but also, if possible, to determine the thermodynamic properties of silver orthoarsenate by measuring the EMF values of the following cells:

$$Ag\left|Ag^{+}\text{-}\beta\text{-alumina}\right|P_{AsH_3},\ P_{O_2},\ Pt \qquad [6.3.1]$$

$$Ag\left|Ag^{+}\text{-}\beta\text{-alumina}\right|\tilde{P}_{As_4O_6},\ \bar{P}_{O_2},\ Pt \qquad [6.3.2]$$

as a function of temperature, P_{AsH_3} concentration (P_{O_2} = const.), $\tilde{P}_{As_4O_6}$ concentration (P_{O_2} = const.) and P_{O_2} concentration (P_{AsH_3} or $\tilde{P}_{As_4O_6}$ = const.).

According to the preliminary analysis based on the literature, the following reactions were expected to take place at the electrodes:

reference: $3Ag = 3Ag^{+} + 3e$ [6.3.3]

working: $3/4\ O_2 + 3e = 3/2\ O^{2-}$ [6.3.4]

$3/2\ O^{2-} + 1/4As_4O_{10}(g) = AsO_4^{3-}$ [6.3.5]

$3Ag^{+} + AsO_4^{3-} = Ag_3AsO_4$ [6.3.6]

Thus, the overall cell reaction would be:

$3Ag + 3/4\ O_2(g) + 1/4As_4O_{10}(g) = Ag_3AsO_4$ [6.3.7]

In addition, assuming arsine is completely oxidized before reaching the surface of the electrolyte and that an equilibrium is established among the supposedly only stable gaseous species of arsenic oxide (i.e. As_4O_6, As_4O_7, As_4O_8, As_4O_9 and As_4O_{10}), we can express the equilibrium concentrations of tetrarsenic pentoxide as:

$$P_{As_4O_{10}} = P^t_{As_4O_x} \cdot K_{6+4} P^2_{O_2} \left(1 + \sum_{i=1}^{4} K_{6+i} P^{i/2}_{O_2}\right)^{-1} \qquad [6.3.8]$$

where K_{6+i} are the equilibrium constants for the reaction:

$$As_4O_6 + i/2\ O_2 = As_4O_{6+i}$$

and $P^t_{As_4O_x}$ is the total pressure of arsenic oxides. With these assumptions the EMF of cells [6.3.1] and [6.3.2] can be expressed as:

$$EMF = -\frac{\Delta G^\circ_{[6.3.7]}}{3F} + \frac{2.3RT}{12F} \log P^t_{As_4O_x} K_{6+4} P^2_{O_2} \left(1 + \sum_{i=1}^{4} K_{6+i} P^2_{O_2}\right)^{-1} P^3_{O_2} \qquad [6.3.9]$$

For the cell [6.3.1] $P^t_{As_4O_x} = 0.25\ P_{AsH_3}$, while for the cell [6.3.2] $P^t_{As_4O_x} = \tilde{P}_{As_4O_6}$ is given by the temperature of the arsenolite bath and calculated by using equation [4.5]. Clearly, for a constant P_{O_2}, EMF should be a linear function of log P_{AsH_3}, or log $P^t_{As_4O_x}$. For a constant P_{AsH_3} the dependence of EMF on log P_{O_2} would indicate the order of the magnitude of K_{6+4} and of other K_{6+i} constants. Finally, the measurement of EMF as a function of temperature would provide the $\Delta H^\circ_{[6.3.7]}$ and $\Delta S^\circ_{[6.3.7]}$ values for the reaction [6.3.7].

The two designs of silver β-alumina sensor, sensor I and sensor II, are shown in Figures 2a and 2b respectively. With sensor I, only arsine was used as the source of arsenic oxide, while with sensor II both arsine and the arsenolite bath were employed.

6.3.1 Activity of silver in the electrolyte

Before equilibrating each sensor with arsine - oxygen - nitrogen mixtures, several exploratory measurements of the silver activity at the surface of the electrolyte were made by measuring the EMF of the cells:

$$Ag \left| Ag^{+}\text{-}\beta\text{-alumina} \right| P_{O_2}(air),\ Pt \qquad [6.3.10]$$

or

$$Ag \left| Ag^{+}\text{-}\beta\text{-alumina} \right| P_{O_2} = 1,\ Pt \qquad [6.3.11]$$

These measurements showed that at temperatures between 673°K and ≈ 825°K, the activity of silver in Ag-β-alumina slightly decreases with temperature, but above 825°K it starts to increase. For the two different designs, sensors I and II, the values of the EMF of both cells, [6.3.10] or [6.3.11], were different by about 40 mV. At 811°K and a flowrate of 0.15 ml/s of oxygen, the EMF values for cell [6.3.11] were 332 mV and 288 mV for the internal and external surface (Figure 2a and Figure 2b) respectively. Such differences are commonly observed for sodium β-alumina tubes (57).

Additional measurements with a new sensor II have led to the following equations for the EMF values of cell [6.3.10] as a function of temperature:

$605°K < T < 805°K$

$$EMF = 795 + 0.25T\ (mV) \qquad [6.3.12]$$

$823°K < T < 980°K$

$$EMF = 498 - 0.25T \text{ (mV)} \qquad [6.3.13]$$

These EMF values indicate that, in air, the activity of silver ion on the (outside) surface of the silver β-alumina tubes varies from 0.0168 at 773°K to 0.083 at 1073°C. These values are important for the evaluation of the sensor sensitivity to arsenic oxide and potential sulphur dioxide contaminant.

6.3.2 Initial sensor equilibration with arsine - formation of Ag_3AsO_4 on the surface

In both cases when arsine was introduced into the system, the sensor responded instantaneously. Initially, the value of EMF decreased, but within several seconds it started to increase. The EMF took 2 to 4 hours to reach a steady value. In this period, a layer of silver orthoarsenate was deposited on the surface of the electrolyte.

6.3.3 Response time

Thereafter, sensor I responded instantaneously to concentration changes and steady values were obtained in about 5-30 minutes, depending on the concentration step. This response time was significantly longer then in the case of $AgZr_2(AsO_4)_3$ and $NaCaAsO_4$, but still reasonable for analytical purposes. It could probably be reduced by decreasing the thickness of the electrolyte.

In the case of sensor II, the response time was comparable to that observed with sensor I, however as will be discussed later, the sensitivity to concentration changes was much lower.

With respect to temperature changes, the response time was relatively short. For a step change of 20°C it took about 20 min to reach a steady EMF value.

6.3.4 Gas flowrates

For practical reasons and based on the results with $AgZr_2(AsO_4)_3$ and $NaCaAsO_4$ electrolytes, the total flowrates were maintained at < 1 ml/s. Several tests showed that at lower arsine concentrations (<70 ppm), the effect of flowrates between 0.3 - 1 ml/s was small. At high arsine concentrations, both sensors were sensitive to the flowrates, particularly for oxygen concentrations below 0.21 atm.

6.3.5 Reproducibility

Sensor I was in operation for more then six weeks. In this period the temperature of the sensor was cycled 3 times between 680 and 910°C either by continuous heating (or cooling) at the rate of 0.5°C/min or in steps, with a given temperature being maintained for several days. During the whole period, for a given temperature and concentration the EMF values were reproducible to within 5 mV.

The reproducibily of sensor II was more difficult to evaluate since the sensor was not operating as well and consequently it was employed for a shorter period of time. Nonetheless, results obtained about 10 days apart were in good agreement with each other.

6.3.6 EMF as a function of P_{AsH_3} or $\tilde{P}_{As_4O_6}$ at P_{O_2} = 0.21 atm

Since the sensitivities of the two sensors to arsenic oxide concentrations were different, the results were treated separately.

6.3.6.1 Sensor I

Figure 9 represents the results obtained for five different temperatures (986, 1008, 1118, 1124 and 1174°K) with a total gas flowrate kept at 1 ml/s. It is clear that the EMF varied as a linear function of log P_{AsH_3} in the range of concentrations studied. However, the slopes of the lines were again double the theoretical, based on equation [6.3.9]. An excellent response was obtained even at temperatures above the melting point of silver orthoarsenates (> 1080°K), although at 1174°K the lower concentration limit was placed at ≈ 15 ppm. On the other hand, an upper concentration limit of ≈ 500 ppm was observed, but this evidently increased with higher oxygen concentrations and lower flowrates.

6.3.6.2a Sensor II - sensitivity to arsine

In comparison with the first sensor, the sensitivity to arsine of sensor II was greatly decreased. In fact, we were only able to obtain a reliable concentration dependence at the lower temperatures (974°K). The results are shown in Figure 10. The results for the higher arsine concentrations were obtained several days after measurements for the lower concentration range and with flowrates of 0.5 ml/s. Although the results for the low concentration range show a scatter, the reproducibility can be considered as good. The slope of the line is again double the theoretical.

In these conditions, the upper concentration limit was ≈ 1000 ppm.

6.3.6.2b Sensor II - sensitivity to arsenic oxide generated by an arsenolite bath

When an arsenolite bath was used as a source of arsenic oxide, an unexpected response was observed. With the sensor at 700°C and the arsenolite bath at 149°C, i.e. the $\tilde{P}_{As_4O_6}$ = 33.3 ppm, the EMF value decreased, instead of increasing and was very sensitive to the flowrate: the higher the flowrate, the higher the EMF decrease. This unexpected concentration dependence effect was reproducible, although after 2-3 hr the EMF values started to drift very slowly to higher EMF. Similarly, the apparent inactivity to As_4O_6 was also observed when a sodium β-alumina probe was tested.

These experiments indicated that as assumed, the pentoxide is the active species in the cell reaction [6.3.7] and that its concentration under the conditions tested was negligibly low. The increase in silver activity as a function of As_4O_6 concentration could only be explained by a different reaction mechanism between silver and As_4O_6, leading however to silver orthoarsenate, by a very slow reaction. The experimental conditions did not assure a fast arsenic pentoxide equilibration.

6.3.7 EMF as a function of P_{O_2} at P_{AsH_3} = const.

6.3.7.1 Sensor I

Figures 11, 12 and 13 represent the EMF values measured as a function of P_{O_2} for P_{AsH_3} equal to 5.3 ppm, 23 ppm and 255 ppm respectively at various temperatures. In these experiments, the flowrates

were also kept at 1 ml/s. Inspection of the figures indicates that the dependence of EMF on P_{O_2} changed with the concentration of arsine. For 5.3 ppm, this dependence is linear with the slope close to the double the theoretical value (with respect to pentoxide as the major species) for P_{O_2} between 1 - 0.015 atm. In the case of 23 ppm arsine the function is evidently polynomial, but at higher P_{O_2} values the straight lines have slopes close to those obtained in the first case. Finally, for 255 ppm arsine the function seems to be linear again, but the slopes are even higher then those for the two first cases.

Table 6 summarizes the values of the observed slopes b of the linear function:

$$EMF = a + b \log P_{O_2} \qquad [6.3.14]$$

6.3.7.2 Sensor II

With respect to sensitivity to arsine, the response of sensor II to changes in P_{O_2} seemed satisfactory, although the functional dependence was different. Figure 14 shows the results obtained for P_{AsH_3} = 5.3 ppm at 923 and 974°K and for P_{AsH_3} = 255 at 1007°K. In this figure it is clear that the EMF is a polynomial function of log P_{O_2}, approaching a linear function as log $P_{O_2} \to 0$. For a better comparison, the slopes of these functions ($P_{O_2} \to 1$) are included in Table 6.

TABLE 6

VALUES OF THE SLOPES b OF THE FUNCTION

$$EMF = a + b \log P_{O_2} \quad (\text{for } P_{O_2} \to 1)$$

Sensor	T	$\frac{2.3RT}{3F}$ [mV]	b [mV]		
			P_{AsH_3} [ppm]		
			5.3	23	255
I	986	65	96	99	146
	1006	66.6	104	104	144
	1038	68.6	---	---	---
	1124	74.3	104	118	140
	1174	77.6	---	108	131
II	923	61.0	51	---	---
	974	64.4	56	---	---
	1007	66.6	---	---	72

6.3.8 EMF as a function of temperature

6.3.8.1 Sensor I

The EMF as a function of temperature was measured for several

P_{AsH_3} and P_{O_2} concentrations and different total gas flowrates. Table 7 indicates the conditions at which the temperature dependence was determined.

TABLE 7

GAS CONCENTRATIONS AND FLOWRATES FOR MEASUREMENTS OF EMF AS A FUNCTION OF TEMPERATURE

P_{AsH_3} x 10^6 [atm]	P_{O_2} [atm]	flowrate [ml/s]
1847	0.63	0.15
36	0.63	0.6
255	0.95	1.0
255	0.21	1.0

The results are plotted in Figure 15 and clearly indicate that the EMF can be expressed as a linear function of temperature, i.e.

$$EMF = a + bT \qquad [6.3.15]$$

However, slope b of this function changes at ≃ 1083°K (≃ 810°C) which apparently corresponds to the melting point of Ag_3AsO_4 (see Table 2).

6.3.8.2 Sensor II

With this sensor, a similar linear dependence of EMF on

temperature was observed but only to 1068°K with P_{AsH_3} = 1847 ppm, P_{O_2} = 0.63 atm and flowrate of 0.15 ml/s. Above 1068°K, a much more rapid EMF decrease was observed. At P_{AsH_3} = 36 ppm, P_{O_2} = 0.63 atm and flowrate of 0.6 ml/s the EMF values decreased linearly with temperature only upto 1023°K. This behavior again reflected the lower sensitivity of sensor II to the arsine concentration and is discussed in the next section together with the other results.

6.3.8.3 Sensor II-2

In order to verify whether the oxidation of arsenic trioxide could be promoted by platinum as a catalyst, a new sensor II was constructed and a 0.5 x 2 cm piece of platinum mesh placed in the gas inlet tube (Figure 2c), close to its end. This sensor was tested with an arsenolite bath (at 148°C) as a source of arsenic oxide i.e.

$\tilde{P}_{As_4O_6}$ = 31.1 ppm and P_{O_2} = 0.21 atm

Starting with an equilibration at 973°K, the sensor did not respond by a significant decrease in EMF as observed earlier, section [6.3.6.2b], but instead started to increase very slowly. It took about 9 hr to reach a steady value of ≃ 70 mV above that of the Ag β-alumina in air. This EMF was slightly dependent on the flowrate. No exact $\tilde{P}_{As_4O_6}$ concentration dependence has been measured, but when the arsenolite bath was cooled to 76°C ($\tilde{P}_{As_4O_6}$ < 0.3 ppm) the EMF decreased by ≃ 65 mV. The sensor was then reequilibrated at 1003°K with $\tilde{P}_{As_4O_6}$ = 31.1 ppm and P_{O_2} 0.21 and the EMF measured as a function of temperature, this being decreased (and then increased) in steps

of about 10°C. The sensitivity of the sensor to any temperature change was relatively slow, but when a steady value of EMF was obtained, it remained constant for up to several hours. At temperatures lower than 843°K (570°C), the EMF started to decrease with decreasing temperature, and 1025°K (753°C) appeared to be the upper temperature limit.

The results are represented in Figure 17. Two regions of linear response were observed: 848° - 940°K, and 940° - 1025°K. The temperature of 940°K at which the slope of the linear function [6.3.15] changes, corresponds most likely to the phase transition of Ag_3AsO_4 (Table 2).

6.3.9 Interpretation of experimental results

All experimental results, sections 6.3.6, 6.3.7, 6.3.8 (and also those for other electrolytes in sections 6.1 and 6.2) suggest that with arsine as a source of arsenic oxide, the electrode reaction involves a gaseous arsenic pentoxide monomer and that the formation of silver orthoarsenate is somehow promoted by the reaction products of arsine oxidation. In this manner, the design of the sensor influences the overall reaction kinetics and plays an important role.

In agreement with the literature and with our own results, arsine can still be assumed to be completely oxidised. However, a whole range of oxide species has to be considered. Thus, the total arsine concentration can be expressed as:

$$P_{AsH_3} = \alpha P_{As_4O_{10}} + \beta P^{\frac{1}{2}}_{As_4O_{10}} + \gamma P^{\frac{1}{4}}_{As_4O_{10}} \qquad [6.3.16]$$

where

$$\alpha = 4\, K_{6+4}^{-1}\, P_{O_2}^{-1}\, (1 + \sum_{i=1}^{4} K_{6+i}\, P_{O_2}^{i/2}) \qquad [6.3.16a]$$

$$\beta = 2\, K_D^{-1/2}\, K_{3+2}^{-1}\, P_{O_2}^{-1}\, (1 + \sum_{i=1}^{2} K_{3+i}\, P_{O_2}^{i/2}) \qquad [6.3.16b]$$

$$\gamma = K_D^{-1/4}\, K_r^{-1/2}\, P_{O_2}^{-1/4} = K_D^{-1/4}\, K_{rd}^{-1/2}\, K_{3+2}^{-1/2}\, P_{O_2}^{1/4} \qquad [6.3.16c]$$

and K_D, K_{3+2}, K_r and K_{rd} are the equilibrium constants for the following gas phase reactions respectively:

$$2As_2O_5 = As_4O_{10} \qquad [6.3.17]$$

$$As_2O_3 + i/2\ O_2 = As_2O_{3+i} \qquad [6.3.18]$$

$$2AsO_2 + 1/2O_2 = As_2O_5 \qquad [6.3.19]$$

$$2AsO_2 = As_2O_3 + 1/2O_2 \qquad [6.3.20]$$

Each of the three terms in equation 6.3.16 represents the total concentration of tetraarsenic, diasernic and monoarsenic oxide species respectively. Obviously, even when P_{O_2} = const., the concentration of $P_{As_4O_{10}}$ could be explicitely expressed as a linear function of P_{As} only, when one of the three groups of molecular species is preponderant. Thus, for:

$$\alpha\, P_{As_4O_{10}} \gg \beta\, P_{As_4O_{10}}^{1/2} + \gamma\, P_{As_4O_{10}}^{1/4} \qquad [6.3.21]$$

a so far generally accepted assumption, $P_{As_4O_{10}}$ would be expressed by

equation [6.3.8] and equation [6.3.9] should hold.

However, when:

$$\beta\ P^{\frac{1}{2}}_{As_4O_{10}} \gg \alpha\ P_{As_4O_{10}} + \gamma\ P^{\frac{1}{4}}_{As_4O_{10}} \qquad [6.3.22]$$

$$P_{As_4O_{10}} = \frac{(P_{As})^2}{\beta} \qquad [6.3.23]$$

In this case when P_{O_2} is constant, the EMF of cell [6.3.1] is given by:

$$EMF = C_{As} + \frac{2.3RT}{6} \log P_{AsH_3} \qquad [6.3.24]$$

where

$$C_{As} = -\frac{\Delta G^\circ_R}{3F} + \frac{2.3RT}{6F} \log \frac{K_D^{1/2}\ K_{3+2}\ P^{5/2}_{O_2}}{2\ (1 + \sum_{i=1}^{2} K_{3+i}\ P^{i/2}_{O_2})} \qquad [6.3.25]$$

In fact, the results in Figures 9 and 10 fit equation [6.3.24] very well. However, it is evident that if equations [6.3.24] and [6.3.25] completely represent the equilibria at the electrode of the cell [6.3.1], when P_{AsH_3} is kept constant, the EMF dependence on P_{O_2} will be expressed by the following equation:

$$EMF = C'_0 + \frac{2.3RT}{6F} \log \frac{K_{3+2}\ P^{5/2}_{O_2}}{(1 + \sum_{i=1}^{2} K_{3+i}\ P^{i/2}_{O_2})} \qquad [6.3.26]$$

where

$$C'_0 = -\frac{\Delta G^\circ_R}{3F} + \frac{2.3RT}{6F} \log K_D^{1/2} + \frac{2.3RT}{6F} \log \frac{P_{AsH_3}}{2} \qquad [6.3.27]$$

The EMF is a linear function of log P_{O_2} only when $\sum_{i=1}^{2} K_{3+i} P_{O_2}^{i/2} \ll 1$ or when $K_{3+2} P_{O_2} \gg K_{3+1} P_{O_2}^{\frac{1}{2}} \gg 1$. In the first case the slope b of the equation:

$$EMF = a + b \log P_{O_2} \qquad [6.3.14]$$

will be equal to $\frac{2.3RT}{12} 5 = 0.0827\ T$ mV, in the second case b should be equal to 0.0496 T mV. In addition, the functional dependence of EMF on log P_{O_2} should be according to equations [6.3.25] and [6.3.26], independent of the value of P_{AsH_3}.

However, our results (Figures 11-14) are not in agreement with the above expectations. Firstly, the expected value of the slope b is aproached only in the case of sensor II for $P_{O_2} > 0.6$ atm (Figure 14). In other cases (Figures 11-13 and Table 6), the values of the slope b seem to be double the expected values. In addition, as the arsine concentration increases (in the case of sensor I) the EMF is more dependent on P_{O_2}. This could only be explained by a local equilibrium controlled by an apparently adsorbed atomic oxygen and small, but significant values of the third term in equation [6.3.20]. Kinetics could be responsible for the participation of monoarsenic species, perhaps an arsenic acid being a precursor to the arsenic oxide formation.

Unlikely as it sounds, the mechanism with an arsenic acid precursor, dissociating to water and arsenic oxides could explain an increased sensitivity of the sensors to arsine as compared to arsenic oxide. Actually, arsenic acid as a precursor to stable solid arsenic trioxide was identified by mass spectrometry in H_2/O_2 flames, into

which $AsCl_3$ was introduced (59).

In view of these complications, the evaluation of ΔG_R° values for reaction [6.3.7] from relatively limited data sets is at present impossible. Nevertheless, by assuming that the logarithmic function of P_{O_2} in equation [6.3.25] and [6.3.26] can in agreement with the experimental results be expressed as:

$$\log \frac{K_{3+2} \, P_{O_2}^{5/2}}{\left(1 + \sum_{i=1}^{2} K_{3+i} \, P_{O_2}^{i/2}\right)} = \log \chi \, P_{O_2}^{3} \qquad [6.3.27]$$

the values of ΔG_{Rx}° defined as:

$$-\Delta G_{Rx}^\circ = -\Delta G_R^\circ + 2.3RT \log K_D^{\chi} \qquad [6.3.28]$$

can be calculated from experimental C_{As} parameters and/or EMF ($P_{O_2} \to 1$) values.

Furthermore, by using the same assumptions, EMF of the cell [6.3.1] can now be written in terms of the enthalpy ΔH_{Rx}° and entropy ΔS_{Rx}° of the cell reaction as:

$$EMF = -\frac{\Delta H^\circ_{Rx}}{3F} + \frac{\Delta S^\circ_{Rx}}{3F} T + \frac{2.3R}{6F} \log \frac{P_{AsH_3} \, P_{O_2}^{3}}{2} T \qquad [6.3.29]$$

Equation [6.3.29] can be devided by T and simplified as:

$$\frac{EMF}{T} = \frac{a}{T} + b \qquad [6.3.30]$$

It is evident that values of parameters a and b obtained from the experimental data can be used to calculate ΔH°_{Rx} and ΔS°_{Rx} values.

Figure 18 represents the values of EMF/T versus 1/T for all concentrations and the two sensors for which the EMF was measured as a function of temperature, between 840 and 1185°K. This figure includes the data for sensor II-2 with an arsenolite bath as a source of arsenic oxide. It is noted that in this case, the value of the slope is significantly lower than that for other data. The values of the slope a for the other data, regardless of the sensor, are identical, except in the case of sensor I with high arsine concentration. The values of slope "a" give the values of ΔH°_{Rx} shown in Table 8. This table includes the values of the intercepts b and values of $b' = b + 0.03305 \log P_{AsH_3} + 0.0992 \log P_{O_2}$. These values of b' yield the estimates of ΔS°_{Rx} which when combined with the values of ΔH°_{Rx}, give the ΔG°_{Rx} of the cell reaction. Such values of ΔG°_{Rx} at 1000°K are listed in the last column of Table 8.

The values can be compared with ΔG°_{Rx1000} calculated from the appropriate ΔH°_{Rx} values and ΔG°_{RxT} obtained from the values of C_{As} in equation [6.3.23] (Figure 9) or of EMF ($P_{O_2} = 1$) extrapolated from Figures 11-14, all listed in Table 9. A difference of more than 10 kcal is observed between the highest and the lowest value of ΔG°_{Rx1000}. Most likely this spread of the estimated values of ΔG°_{Rx} is attributable to a different regime of reaction kinetics for the two different sensor designs and to the unknown values of $\log \chi$. These differencies are apparently also reflected in the calculated values of ΔH°_{Rx}.

TABLE 8

VALUES OF THE PARAMETERS a AND b IN EQUATION [6.3.27] AND CORRESPONDING ΔH°_{Rx} VALUES AND ESTIMATES OF $\Delta G^{\circ}_{Rx1000}$ FOR THE CELLS [6.3.1] and [6.3.2]

SENSOR	CONDITIONS							
	P_{AsH_3} [ppm]	P_{O_2} [atm]	flowrate [ml/s]	a [V]	$-\Delta H^{\circ}_{Rx}$ [kcal]	- b [mV]	- b' [mV]	$-\Delta G^{\circ}_{Rx1000}$ [kcal]
I	1847	0.6	0.15	1.74[1]	120.4	1.1850	1.0714	46.3
I	36	0.6	0.6			1.1865	1.0163	43.9
I	255	0.95	1.0			1.1085	0.9841	46.1
I	255	0.21	1.0	1.65[1]	114.2	1.2035	1.0141	44.0
II	1847	0.6	0.15			1.2280	1.1144	37.1
II	36	0.6	0.6			1.2670	1.0968	38.3
II-2	31.1*	0.21	0.5	1.32[1]	91.3	1.000	0.8003	35.9
				1.42[2]	98.2	1.1100	0.9100	35.2
I	1847	0.6	0.15	1.2[3]	83.0	0.6960	0.5824	(42.7)
I	36	0.6	0.6	1.2[3]	83.0	0.7740	0.6038	(41.2)

1: temperature range 953 - 1083°K
2: temperature range 850 - 953°K
3: temperature range 1183 - 1183°K
*: $\bar{p}_{As_4O_6}$

TABLE 9

ESTIMATES OF ΔG°_{Rx} values for the reaction of the cell [6.3.1] AND [6.3.2]

SOURCE						
SENSOR	FUNCTION	P_{AsH_3} [ppm]	P_{O_2} [atm]	T [°K]	ΔG°_{RxT} [kcal]	$\Delta G^{\circ}_{Rx1000}$ [kcal]
I	EMF vs P_{O_2}	5.3		986	44.1	43.1
	"	5.3		1008	43.4	44.0
	"	23.0		986	44.4	43.4
	"	23.0		1008	43.4	44.0
	"	255		986	47.4	46.5
	"	255		1008	46.1	46.6
	"	255		1032	43.4	45.6
II	"	5.3		974	39.5	37.5
	"	255		1007	37.4	37.9
II	EMF vs P_{AsH_3}		0.21	974	37.9	35.9
I	"		0.21	986	44.7	43.7
I	"		0.21	1008	42.4	43.0
I	"		0.21	1118	37.0	(42.6)
I	"			1124	36.8	(42.6)
I	EMF vs P_{O_2}	255		1173	35.8	(43.8)
I	"	23		1173	34.4	(42.6)
		23		1124	36.6	(42.0)

It is evident that a further study of the complex arsenic oxide systems is necessary in order to ascertain the exact reactions represented by a given set of thermodynamic data.

Regardless of the uncertainty in the value of ΔG°_{Rx}, a more accurate estimation of the selectivity of the silver β-alumina based sensor to arsenic oxide as compared with sulphur dioxide can now be made.

For example, at 1000°K, based on our results the activity of silver in silver β-alumina in air is ≈ 0.053. Thus, according to thermodynamic calculations on the F*A*C*T system (60), silver β-alumina could function as a sulphur dioxide sensor only for $P_{SO_2} > 0.8 \times 10^{-2}$ atm. The experimental data for arsenic oxide indicate $P_{As} > 10^{-4}$ atm as the most conservative estimate of the sensitivity for arsenic (oxide). Evidently, at least a 100 fold selectivity of silver β-alumina based sensor to arsenic oxide can be expected.

6.4 Evaluation of the sodium β-alumina solid electrolyte

Unlike sodium calcium orthoarsenate (and sodium orthoarsenate), sodium β-alumina offers the possibility of using air as a reference. Thus, the objective of this evaluation was not only to analyse the suitability of sodium β-alumina as an arsenic oxide sensor, but also to obtain more details concerning the actual electrode reactions involving either arsine or arsenic trioxide. To meet this objective, the EMF values of the cells:

$$\text{Pt, air} \left| \text{Na } \beta\text{-alumina} \right| P_{AsH_3}, P_{O_2}, \text{Pt} \qquad [6.4.1]$$

CDT
Centre de
Développement
Technologique
École Polytechnique
de Montréal

and

$$Pt, air \left| Na\ \beta\text{-alumina} \right| \tilde{P}_{As_4O_6}, P_{O_2}, Pt \qquad [6.4.2]$$

were measured as a function of P_{AsH_3} or $\tilde{P}_{As_4O_6}$ concentration (P_{O_2} = const.) and P_{O_2} concentration (P_{AsH_3} = const.) at 1075 and 1025°K. Only a limited number of experiments were carried out but they confirmed the results obtained with the $NaCaAsO_4$ electrolyte (section 6.2).

6.4.1 Air as a reference electrode

Initial measurements of the EMF of the cell:

$$Pt, air \left| Na\ \beta\text{-alumina} \right| air, Pt \qquad [6.4.3]$$

at several temperatures in the range of 973 to 1073°K and at various flowrates of air indicated that the sodium activity at the two surfaces of the electrolyte tube (the reference electrode - inner surface, the working electrode - outer surface) was not the same and that it was highly sensitive to flowrates. This was also observed by Dubreuil (57). Nevertheless, by keeping the flowrates identical (0.5 ml/s) at the reference (the inner surface) electrode and the working (the outer surface) electrode, EMF values lower than 15 mV, constant within 3 mV for several hours was obtained for cell [6.4.3] at 1075°K.

6.4.2 Initial sensor equilibration with arsenic trioxide or arsine

The initial experiments with arsenic trioxide (31.1 ppm) vapor generated in the arsenolite bath kept at 148°C were negative. Upon introduction of arsenic trioxide to the sensor, the value of EMF

decreased by ≈ 15 mV and within several minutes returned to the initial value which stayed constant for 2 hr. It was therefore concluded that the arsenic trioxide is not oxidized fast enough to assure a positive response of the sensor to its concentration.

With arsine (as a source of arsenic oxide) at 501 ppm and P_{O_2} = 0.9 atm, the EMF of the sensor started to increase immediately and within 5.5 hr a steady value was obtained. This value remained fairly reproducible (within 10 mV) for 3 days.

6.4.3 Response time

The response time to concentration and temperature changes was slightly longer then in the case of silver β-alumina, but steady values were normally established within 30 min. This compares very well with the response time observed by Itoh et al (17) who used sodium β-alumina as a sensor for SO_2 gas.

6.4.4 Gas flowrates

Cell [6.4.1] was found to be much less sensitive to flowrates than cell [6.4.3]. At 802°C and P_{O_2} = 0.21, the EMF values would change by ≈ 5 mV when the flowrate was changed from 0.3 to 1.2 ml/s. For the flowrate change from 0.5 to 1 ml/s the effect of the flowrate was less then 3 mV. The cell was more sensitive to flowrates when P_{O_2} > 0.6 and P_{AsH_3} > 300 ppm.

6.4.5 Reproducibility

Over a short testing period the reproducibility of the EMF was found to be good. On a single day, values were reproducible to within 5 mV. The overall reproducibility over several days was less than 20 mV.

6.4.6 EMF as a function of P_{AsH_3} at P_{O_2} = 0.21 atm

The results for 1075°K and 1025°K, each obtained over the period of two days, are shown in Figure 19. Both sets of data show a linear dependence of EMF on log P_{AsH_3}. However, as found in the case of the $NaCaAsO_4$ electrolyte, the different slopes (52 mV at 1025°K and 71.5 mV at 1075°K) would suggest a different electrode reaction. While the value of the slope at 1025°K seems to agree very well with the theoretical value (50.8 mV) for the formation of pyroarsenate, if we assume the arsenic pentoxide to be a monomer, i.e.

$$4Na + As_2O_5 + O_2 = Na_4As_2O_7 \qquad [6.4.4]$$

the value of the slope at 1075°K is much too high and would only be compatible with the following stoichiometry:

$$3Na + AsO_2 + O_2 = Na_3AsO_4 \qquad [6.4.5]$$

The theoretical value of the slope for the formation of sodium ortho-arsenate via arsenic pentoxide monomer would be 35.5 mV.

Unlike the case of silver β-alumina, no upper concentration limit (up to 3960 ppm arsine) was observed at either temperature.

6.4.7 EMF as a function of P_{O_2} at P_{AsH_3} = const

At 1075°K, the EMF was measured as a function of P_{O_2} at higher arsine concentrations (P_{AsH_3} = 301 ppm and 502 ppm), while at 1025°K the same measurements were carried out for lower arsine concentrations (P_{AsH_3} = 5 ppm and 9.8 ppm). The results are shown in Figure 20.

As in the case of silver β-alumina, at higher arsine concentrations, the EMF values of cell [6.4.1] were much more dependent on the oxygen concentration than at lower concentrations.

6.4.8 EMF as a function of temperature

EMF values, as a function of temperature were measured at P_{AsH_3} = 502 ppm, P_{O_2} = 0.21 atm and flowrate = 0.5 ml/s by heating the cell at the rate of 0.5°C/min and then by cooling at the same rate, in the range of temperatures 1075 - 1113°K and 1113° - 955°K. An almost identical temperature dependence was observed for heating and cooling. In both cases, a change in the temperature dependence was observed at 1023°, 1113° and 1165°K. These changes are apparently associated with the changing stability of the equilibria involving sodium pyroarsenate and sodium orthoarsenate as well as various arsenic oxides.

6.4.9 Interpretation of the results

The EMF value of the cell [6.4.1] can be expressed as:

$$EMF = E^r - E^w = \frac{\Delta G^\circ_{Na_2O}}{2F} + \frac{2.3RT}{2F} \log a^\beta_{Na_2O} - \frac{2.3RT}{4F} \log P_{O_2} -$$

CDT
Centre de
Développement
Technologique
École Polytechnique
de Montréal

$$- \frac{\Delta G^{\circ}_{\text{Na-ars.}}}{nF} - \frac{2.3RT}{nF} \log P^{I}_{O_2} - \frac{2.3RT}{nF} \log P^{J}_{As_2O_5} \qquad [6.4.6]$$

where the subscript Na-ars. in equation [6.4.6] indicates Na-arsenate, i.e. Na-pyroarsenate or Na orthoarsenate.

By using literature values for $\Delta G^{\circ}_{Na_2O}$ (58) and for $\log a^{\beta}_{Na_2O}$ (49) the value of E^{r} was calculated as:

$$E^{r} = -3241.6 + 0.6986T \text{ [mV]} \qquad [6.4.7]$$

As shown in section 6.2, E^{w} appears to depend on the electrode reaction, i.e. formation of pyroarsenate, or orthoarsenate. Futhermore, based on the experimental results, it is assumed that the arsenic pentoxide monomer is the important species. In the expression for E^{w}, the values of n, I and J would change according to the cell reaction, and $P_{As_2O_5}$ can be expressed by using equation [6.3.16] relating a total arsenic concentration and partial concentrations of individual oxide species.

Thus, for the case of (sodium) pyroarsenate formation (equation [6.4.4]) equation [6.4.6] could be rewritten as:

$$EMF = E^{r} - C'_{As} + \frac{2.3RT}{4F} \log P_{AsH_3} \qquad [6.4.7]$$

where

$$C'_{As} = - \frac{\Delta G^{\circ}_{Na_4As_2O_7}}{4F} + \frac{2.3RT}{4F} \log \frac{K_D^{1/2} K_{3+2} P^{2}_{O_2}}{2\left(1 + \sum_{i=1}^{2} K_{3+i} P^{i/2}_{O_2}\right)} \qquad [6.4.8]$$

In addition, for $K_{3+2} P_{O_2}^2 >> K_{3+1} P_{O_2}^{1/2} >> 1$ the equation [6.4.8] could be simplified as:

$$C'_{As} = \frac{\Delta \bar{G}^\circ_{Na_4 As_2 O_7}}{4F} + \frac{2.3RT}{4F} \log P_{O_2} \qquad [6.4.9]$$

For 1025°K, both sets of experimental data (Figures 19 and 20) seem to be in a good agreement with equation [6.4.7] and [6.4.9] respectively.

On the other hand, for 1075°K the results limited to high arsine concentrations seem to conform with the following equations:

$$EMF = E^r - C'_{As} + \frac{2.3RT}{3F} \log P_{AsH_3} \qquad [6.4.10]$$

with

$$C'_{As} = \frac{\Delta \bar{G}^\circ_{Na_3 AsO_4}}{3F} + \frac{2.3RT}{3F} \log P_{O_2} \qquad [6.4.11]$$

when $P_{O_2} \to 1$

However, a possibility that at lower P_{AsH_3} concentrations the data would fit the equations [6.4.7] and [6.4.8] or that similar to [6.3.24] and [6.3.25] can not be excluded.

It is therefore interesting to compare the estimates of ΔG°_{Rp} and ΔG°_{Ro} values, (for the formation of pyroarsenate and orthoarsenate respectively), calculated from the values of C'_{As} and

$C'_{As} + \frac{RT}{n} \log P_{AsH_3}$ extrapolated for $P_{AsH_3} = 1$ atm and $P_{O_2} = 1$ atm respectively. These are collected in Table 10. Both sets of these estimates seem to be reasonable.

While these results do not appear to be in agreement with those obtained with the $NaCaAsO_4$ electrolyte, they are not contradictory and well reflect some similarities with the results obtained with the silver β-alumina electrolyte.

The apparent insensivity of the sodium β-alumina to As_4O_6 could be explained by an insufficient catalysis required to oxidize arsenic trioxide to arsenic pentoxide.

TABLE 10

ESTIMATES OF $\Delta G^\circ_{Na\text{-}ars.}$ VALUES FOR THE REACTION(S) OF THE CELL [6.4.1]

FUNCTION	P_{O_2} [atm]	P_{AsH_3} [ppm]	T [°K]	$-\Delta G^\circ_{Rp}$ [kcal]	ΔG°_{Ro} [kcal]
E vs P_{AsH_3}	0.21	5-500	1025	323.7	
E vs P_{O_2}	0.04-0.95	5.3	1025	323.2	
	0.04-0.95	9.8	1025	321.5	
E vs P_{AsH_3}	0.21	266-3966	1075	320.5	248.7
E vs P_{O_2}	1.04-0.95	301	1075	327.6	249.1
		502	1075	327.8	249.0

ΔG°_{Rp} : ΔG° for the formation of pyroarsenate.

ΔG°_{Ro} : ΔG° for the formation of orthoarsenate.

7. CONCLUSIONS

Both sodium-conducting and silver-conducting solid electrolytes were found to be suitable as membranes in potentiometric sensors for arsenic oxides when arsine was used as a source of the oxides.

In the case of silver β-alumina (and silver zirconium arsenate), the temperature range of linear EMF response to log P_{AsH_3} was ≈ 680 to 810°C with the optimum at 740°C. At these temperatures, concentrations of 5 to 1000 ppm of arsine in air could be detected. For this temperature and concentration range and with P_{O_2} = 0.21 atm, the EMF of a silver β-alumina based sensor obeyed the following equation:

$$EMF = \text{const.} + 0.033T \log P_{AsH_3}$$

Silver orthoarsenate was formed on the surface of the silver conducting electrolyte, when in contact with arsine-oxygen-nitrogen mixtures.

In the case of sodium conducting electrolytes, the temperature range of applicability could be extended to higher temperatures. However, the slope of the linear function relating EMF and log P_{AsH_3} will change at ≈ 750°C.

The oxidation of arsine (or arsenic) apparently proceeds by a complex mechanism which must be responsible for an increased sensitivity of the electrolytes to arsine-oxygen-nitrogen mixtures as compared to arsenic oxide-air mixtures. The oxidation of gaseous arsenic trioxide to arsenic pentoxide requires a very efficient catalyst.

A gaseous system containing arsenic and oxygen is far more complex than generally believed. At temperatures above 600°C and at higher oxygen concentrations, the concentrations of species As_2O_{3+i} must be significant.

Due to the complexity of the arsenic oxide(s) system, the determination of thermodynamic stability constants is very difficult, but feasible when coupled with other methods such as, for example, proposed by Skeaff (25).

The apparent thermal stability constants for silver ortho-arsenate evaluated from the experimental results with silver β-alumina electrolyte indicate a significantly higher stability compared to silver sulphate, which permits an estimate of an approximately 100 fold higher selectivity of silver β-alumina electrolyte to arsenic oxide at 730°C.

The positive results obtained in this study with an arsine-oxygen-nitrogen system indicate that a reliable potentiometric sensor suitable for industrial applications could be developed.

To determine reliable thermodynamic data for arsenic-based compounds, the chemistry of arsenic oxidation must be better understood and the relevant thermodynamic constants determined.

8. SUGGESTIONS FOR FURTHER WORK

- Determine the actual electrode reactions when arsenolite is the source of arsenic oxides.

- Develop an appropriate catalyst to improve the sensor response to arsenic oxides.

- Determine the decomposition equilibrium vapor pressure of arsenic pentoxide over a solid arsenic pentoxide.

- Reevaluate the thermodynamic constant for the formation of silver orthoarsenate and possibly of other arsenates such as Ni and Cu arsenates.

In order to complete the development of a practical probe for monitoring gaseous arsenic oxides, the following work is required:

(i) Evaluation of the selectivity of the probe in the presence of the gaseous contaminants SO_2, H_2O and CO_2.

(ii) Determination of the stability and reproducibility of the probe as a function of time with respect to the different electrolytes.

(iii) Optimization of the cell design in order to simplify the construction and reduce the response time.

The unexpected high sensitivity of the solid electrolytes to arsine concentrations, as compared to gaseous arsenic oxide

concentrations, should be exploited. Detection of arsine in air in the order of 0.05 ppm or less seems quite possible. The low cost of a simple solid-state arsine detector would provide an extremely attractive alternative to the present industrial sensors which are based upon the photoluminescence of arsine oxidation by ozone and can cost upwards of $10,000.

With the knowledge contained in this report, the development of a practical arsine detector to be used in industry could be achieved in a relatively short period of time. The chances of producing a simple and reliable detector are good. The following tasks would complete the development and characterization of the arsine probe:

(i) Determination of the lower limit of arsine sensitivity as a function of temperature for the different electrolytes.

(ii) Determination of the stability (reproducibility) as a function of time.

(iii) Characterization of the selectivity of arsine with respect to contaminants such as H_2, H_2O.

(iv) Modification of the design for use in the industrial environment.

9. REFERENCES

1) I.J. Weisenberg, P.S. Bakshi and A.E. Vervaert, Journal of Metals, Oct., 38 (1979).

2) N. Chakraborti and D.C. Lynch, Metall. Trans., 14B, 239 (1983).

3) H. Tuovinen and P. Sekala, TMS Paper Selection, Paper N° A82-4.

4) M. Gauthier, A. Chamberland and A. Bélanger, NATO Advanced Study Inst., Electrode Processes in Solid State Ionics, Ajaccio, Corsica, (1975).

5) M. Gauthier, A. Bélanger, Y. Meas and M. Kleitz, "Solid Electrolytes", Ch. 29, p. 497, Ed. P. Hagenmuller and W. Van Gool, Academic Press, New York (1978).

6) M. Gauthier and A. Chamberland, J. Electrochem. Soc., 124, 1579 (1977).

7) M. Gauthier, A. Bélanger, D. Fauteux, C.W. Bale and R. Côté, Proceedings of the International Meeting on Chemical Sensors (Fukuoka, Sept. 1983), Elsevier (1983), p. 353.

8) R. Côté, C.W. and M. Gauthier, J. Electrochem. Soc., 131, 63 (1984).

9) V. Demuysère and C.W. Bale, Solid State Ionics, 9 and 10, 1285-90 (1983).

10) M. Gauthier and C.W. Bale, Metall. Trans., 14B, 117 (1983).

11) C.W. Bale and G. Poncet, Submitted to Can. Met. Quart., June (1985).

12) K.T. Jacob and D. Bhogesware Rao, J. Electrochem. Soc., 126, 1842 (1979).

13) N. Imanaka, G. Adachi and J. Shiokawa, Proceedings of the International Meeting on Chemical Sensors (Fukuoka, September 1983), Elsevier, (1983), p. 348.

14) Q.G. Liu and W.L. Worrell, Chemical Metallurgy - A Tribute to Carl Wagner, The Metall. Soc., Warrington PA, (1981), p. 43.

15) Q.G. Liu and W.L. Worrell, U.S. Patent Appl. Ser. N° 3303, 320, September 17 (1981).

16) W.L. Worrell and Q.G. Liu, J. Electroanal. Chem., 168, 355 (1984).

17) Y.Saito, T. Maruyama, Y. Matsumoto and Y. Yono, Proceedings of the International Meeting on Chemical Sensors (Fukuoka, September 1983), Elsevier (1983), p. 326.

18) M. Itoh, E. Sugimoto and T. Kozuka, Trans. Jap. Instit, Metals, 25, 504 (1984).

19) D.E. Williams, Brit. U.K. Pat. Appl. G.B. 2, 119, 933 (1983).

20) M. Gauthier, B. Bellemare and A. Bélanger, J. Electrochem. Soc., 128, 371 (1981).

21) P.J. Durrant and B. Durrant, Introduction to Advanced Inorganic Chemistry. Logmans (1962), Chapter on Arsenic.

22) R.D. Brittain, K.H. Law and D.L. Hildenbrand, J. Phys. Chem., 86, 5072 (1982).

23) R.G. Behrens and G.M. Rosenblatt, J. Chem. Thermodynamics, 4, 175 (1972).

24) J.J. Murray, R.F. Pottie and C. Pupp, Can. J. Chem., 52, 557 (1974).

25) J.M. Skeaff, P.R. Mainwaring and J.L. Speelman, Can. Met. Quart., 24 (4), 349 (1985); 1985 AIME-CIM Extract. and Process Metall. Meet., Nov. 1985, San Diego.

26) H. Guérin and R. Boulitrop, C.R. Acad. Sci., 236, 83 (1953).

27) A.N. Polukarov, M. Zh. Makhmetov and E.A. Buketov, Zhurnal Fiz. Khim., 45, 2688 (1971).

28) Von V. Plies and M. Jansen, Z. Anorg. Allg. Chem., 497, 185 (1983).

29) H. Barten and E.H.P. Cordfunke, Thermochim. Acta, 80, 221 (1984).

30) A.I. Volkov and I.N. Sveshnikova, Izv. Akad. Nauk SSSR, Neorg. Mater., 20, (12), 1969 (1984).

CDT
Centre de
Développement
Technologique
École Polytechnique
de Montréal

31) M.F. Fraser, J. Phys. Chem., 88, 3383 (1984).

32) M.E. Fraser and D.H. Stedman, J. Chem. Soc. Faraday Trans., I, 79, 527 (1983).

33) J. Schoomen and P.H. Bottelberghs, Ch. 20 in "Solid Electrolytes", Ed. P. Hagennmuller and W. Van Gool, Academic Press, New York (1978), p.335.

34) Y.Y. Yao and J.T. Kummer, J. Inorg. Nucl. Chem., 29, 2453 (1967).

35) M.S. Whittingham and R.A. Huggins, J. Electrochem. Soc., 118, 1, (1971).

36) M. Zahir, R. Olazcuaga and P. Hagenmuller, Materials Letters, 2, 124 (1984).

37) P. Tarte, J. Inorg. Nucl. Chem., 29, 915 (1967).

38) M. Pallazi and F. Rémy, Bull. Soc. Chim. France, 2796 (1971).

39) N. Ariguib-Kbir and H. Guérin, Bull. Soc. Chim. France, 863 (1973).

40) H.H. Paques-Ledent, J. Inorg. Nucl. Chem., 38, 215 (1976).

41) N.G. Chernorukov, I.A. Korshunov and T.V. Prokof'eva, Kristallografiya, 23, 844 (1978).

42) K. Tennakone, J. Solid State Chem., 49, 256 (1983).

43) H. Guérin, J. Masson, P. Mattrat, R. Boulitrop, C. Duc-Maugé, R. Martin and R. Mars, Bull. Soc. Chim. France, 440 (1953).

44) P.N. Namboodiri, V.V. Deshpande and K.S. Venkateswarlu, Thermochim. Acta, 60, 55 (1983).

45) L.G. Gorokhova, M. Zh. Makhmetov and V.P. Malyshev, Kompleksnoe Ispol'zovanie Mineral'novo Syrya, 2, 30 (1984).

46) B.K. Kasenov, C.M. Isabaev and A.N. Polukarov, Zh. Fiz. Khim., 53, 2173 (1979).

47) C.M. Isabaev, E.A. Buketov and B.K. Kasenov, Zh. Neorg. Khim., 27, 3163 (1982).

48) W.W. Liang and J.F. Elliott, J. Electrochem. Soc., 123, 617 (1976).

49) A. Dubreuil, M. Malenfant and A.D. Pelton, J. Electrochem. Soc., 128, 2006 (1981).

50) M. Sato, Ch. 3, p. 43, "Research Techniques for High Pressure and High Temperature", Ed. G.C. Ulmer, Springer-Verlag (1971).

51) M. Itoh, K. Kimura and Z. Kozuka, Trans. Jap. Inst. Metals, 26, 353 (1985).

52) P.D. Garn. Thermoanalytical Methods of Investigation, Academic press (1965), p. 43.

53) P.N. Namboodiri, V.V. Deshpande and K.S. Venkateswarlu, Thermochim. Acta, 60, 47 (1983).

54) P.N. Namboodiri, V.V. Deshpande and K.S. Venkateswarlu, Indian J. Chem., 23A, 345 (1984).

55) J.P. Holman, Experimental Methods for Engineers, 4th Ed., McGraw-Hill, (1984) Chapter 8.

56) J. Kirchnerova and C.W. Bale, Proceedings of the Symposium on Quality Control in Nonferrous Pyrometallurgical Processes; 24th Annual Conference of Metallurgists, August 18-21 (1985), p.207.

57) A. Dubreuil, Private Communication.

58) C.B. Alcock and G.P. Stavropoulos, Can. Met. Quat., 10, 257 (1971).

59) M. Farber and R.D. Srivastava, Combust. Flame, 25, 101 (1975).

60) C.W. Bale, A.D. Pelton and W.T. Thompson, "F*A*C*T" - User's Manual, May 1985, McGill University / Ecole Polytechnique.

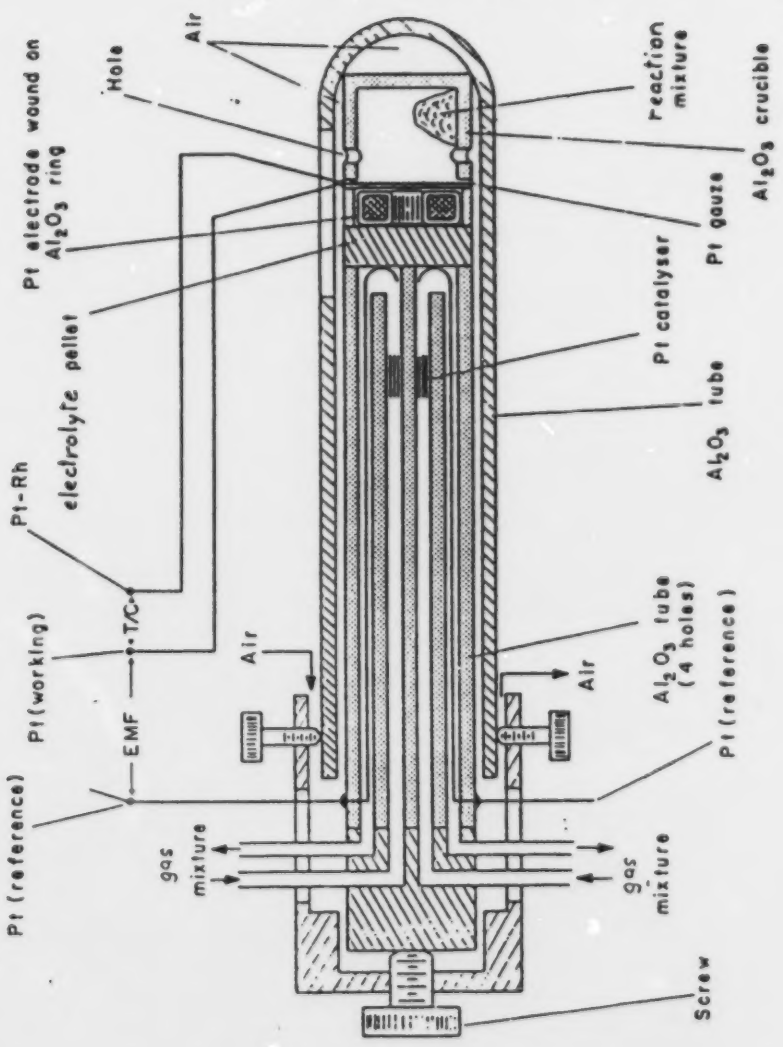

Figure 1: Potentiometric sensor for use with solid electrolyte pellets

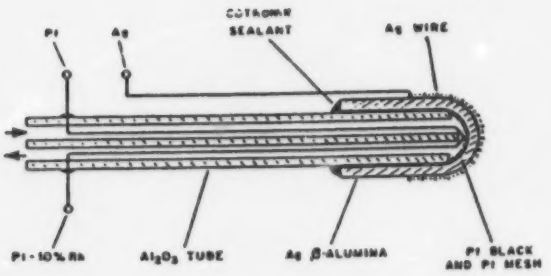

Figure 2a: Sensor I with the reference on the outside

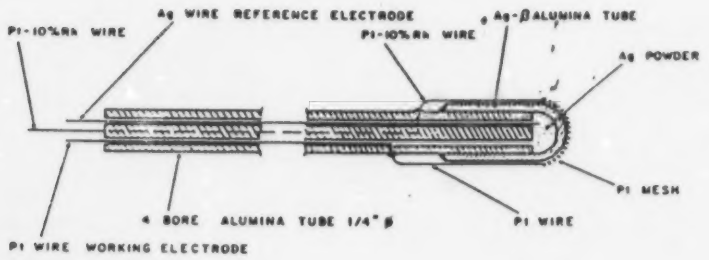

Figure 2b: Sensor II with the reference on the inside

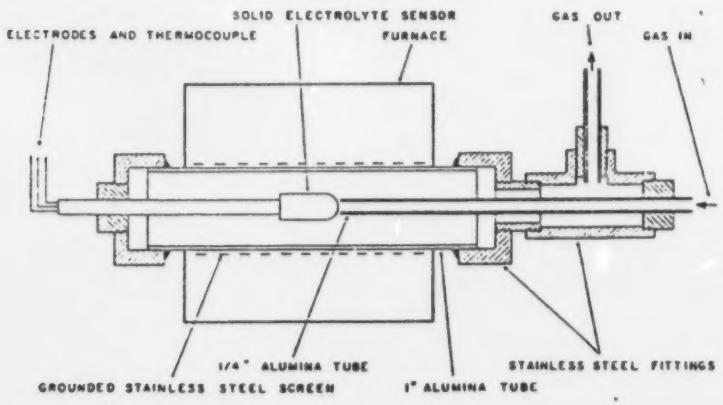

Figure 2c: Complete assembly

Figure 2: Experimental assembly with a potentiometric sensor comprising a solid electrolyte closed-end tube

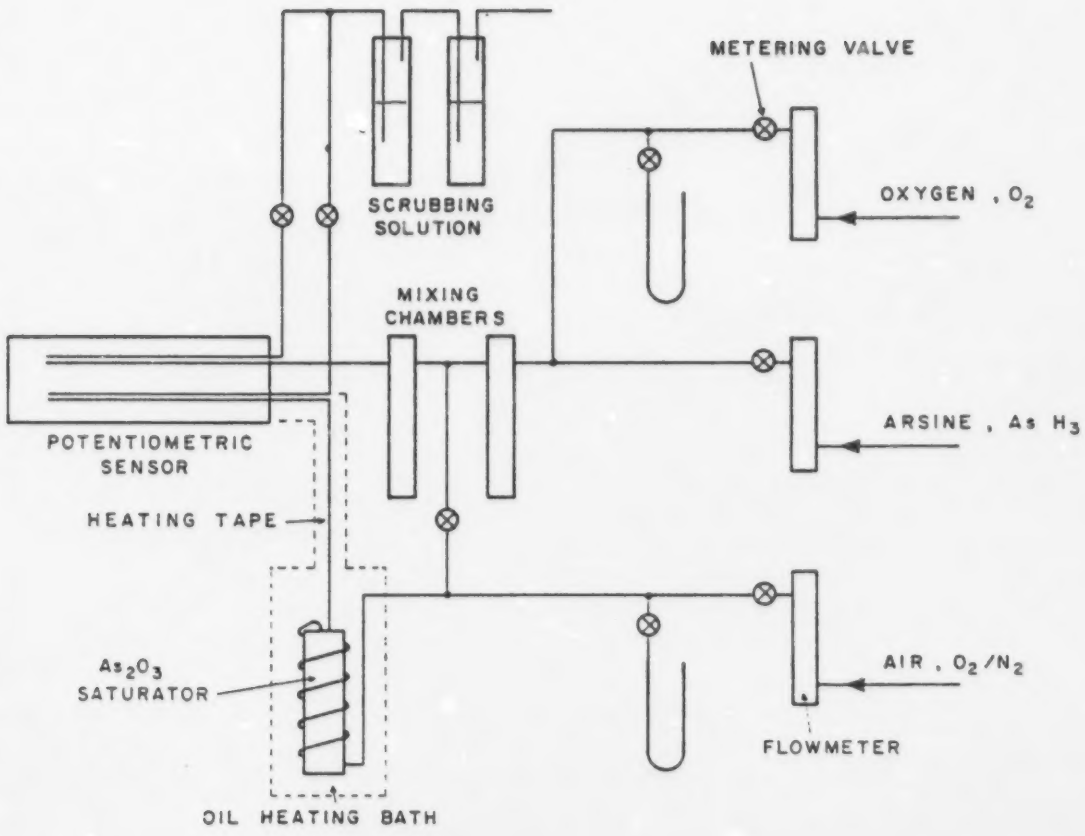

Figure 3: Gas mixing train

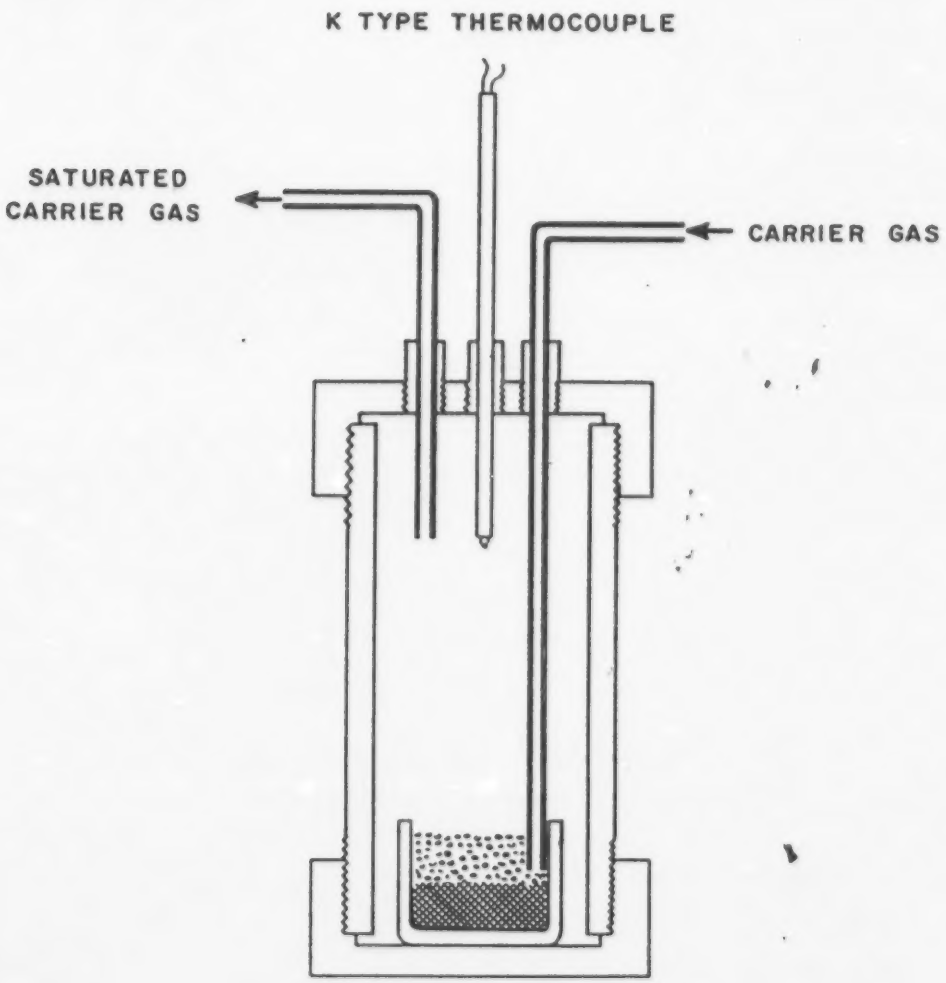

Figure 4: Arsenolite saturator

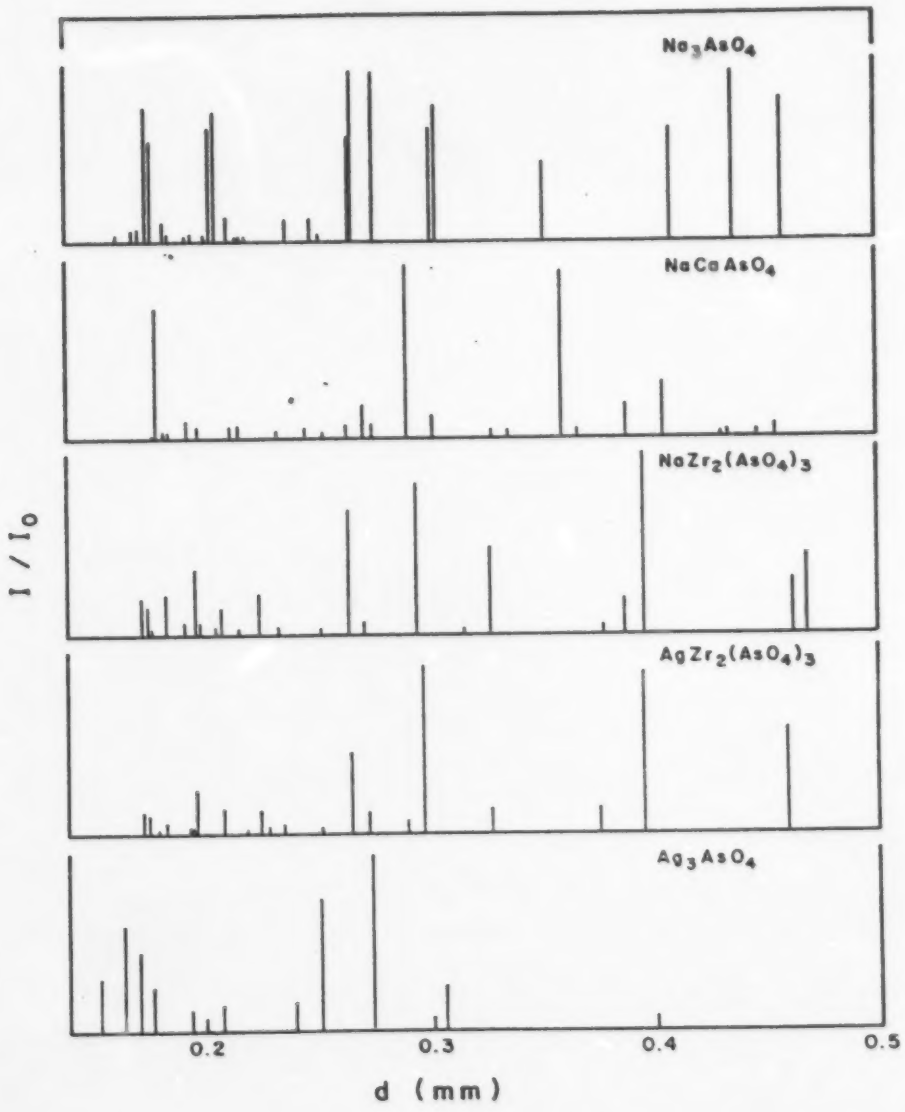

Figure 5: X-ray spectra of the prepared solid electrolytes

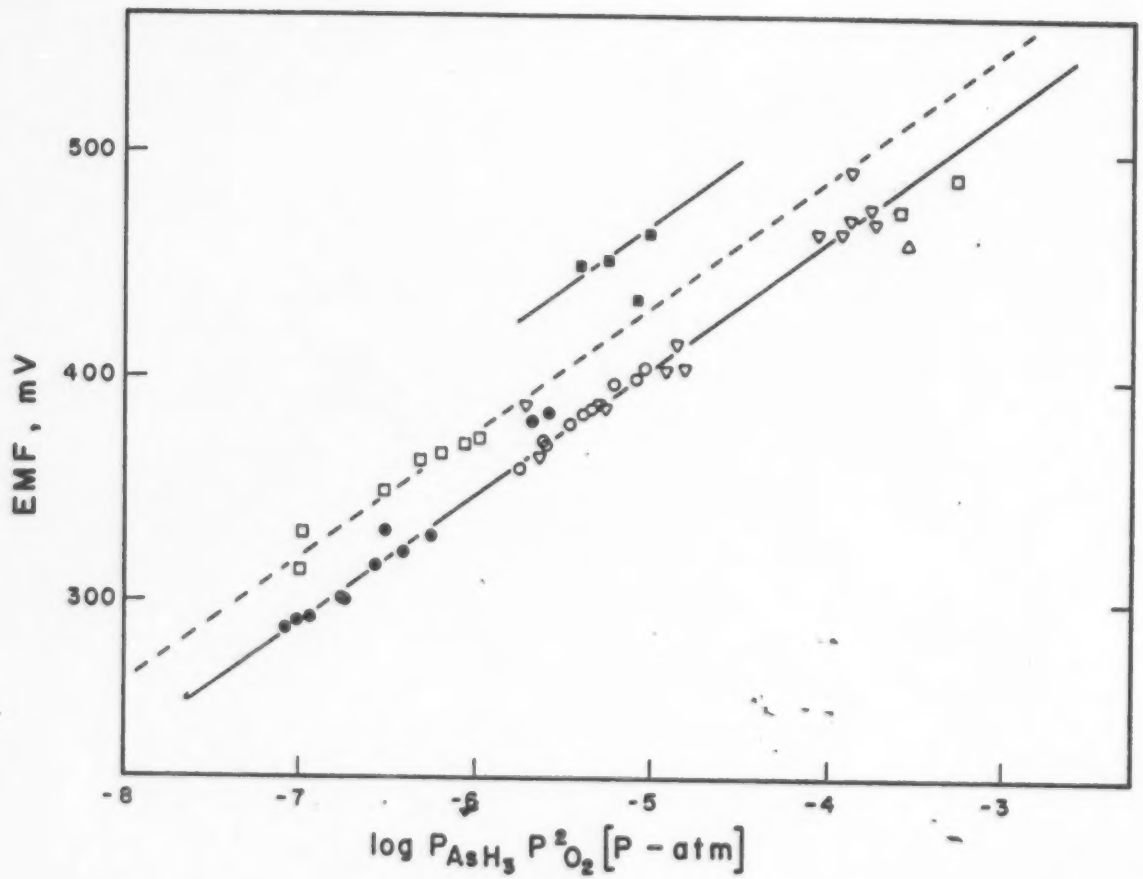

Figure 6: EMF as a function of log $P_{AsH_3} P_{O_2}{}^{\frac{1}{2}}$ [P = atm] for the $AgZr_2(AsO_4)_3$ electrolyte at 985°K. The different points correspond to different days of measurement and/or to different flowrates

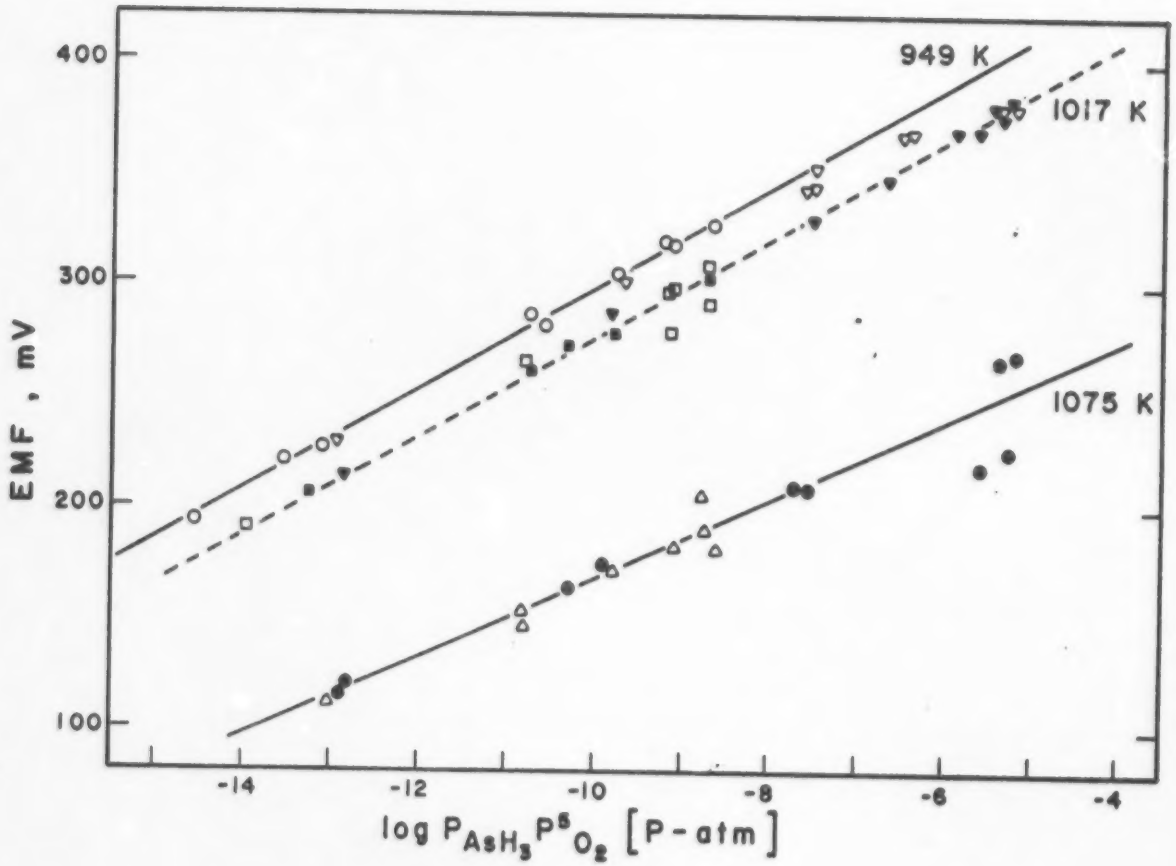

Figure 7: EMF as a function of log $P_{AsH_3} P_{O_2}^{5}$ [P = atm] for the $NaCaAsO_4$ electrolyte at 949°, 1017° and 1075°K. Reference gas concentration: $P_{As_4O_6}$ = 1.3 ppm and P_{O_2} = 0.21 atm. Gas mixtures prepared by mixing arsine/nitrogen with either oxygen or air

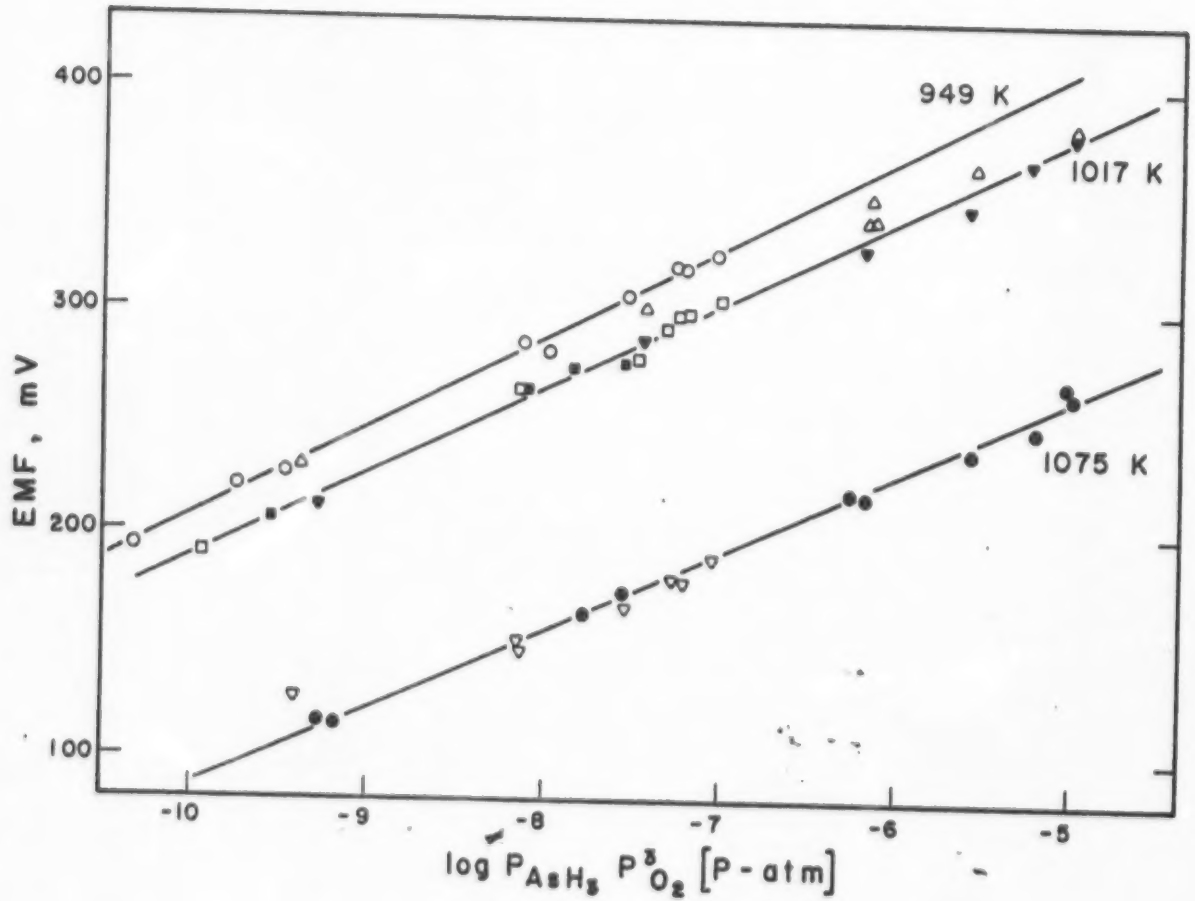

Figure 8: EMF as a function of log $P_{AsH_3} P_{O_2}^{\ 3}$ [P = atm] for the $NaCaAsO_4$ electrolyte at 949°, 1017° and 1075°K. Reference gas concentration: $\tilde{P}_{As_4O_6}$ = 1.3 ppm and P_{O_2} = 0.21 atm. Gas mixtures prepared by mixing arsine/nitrogen with either oxygen or air

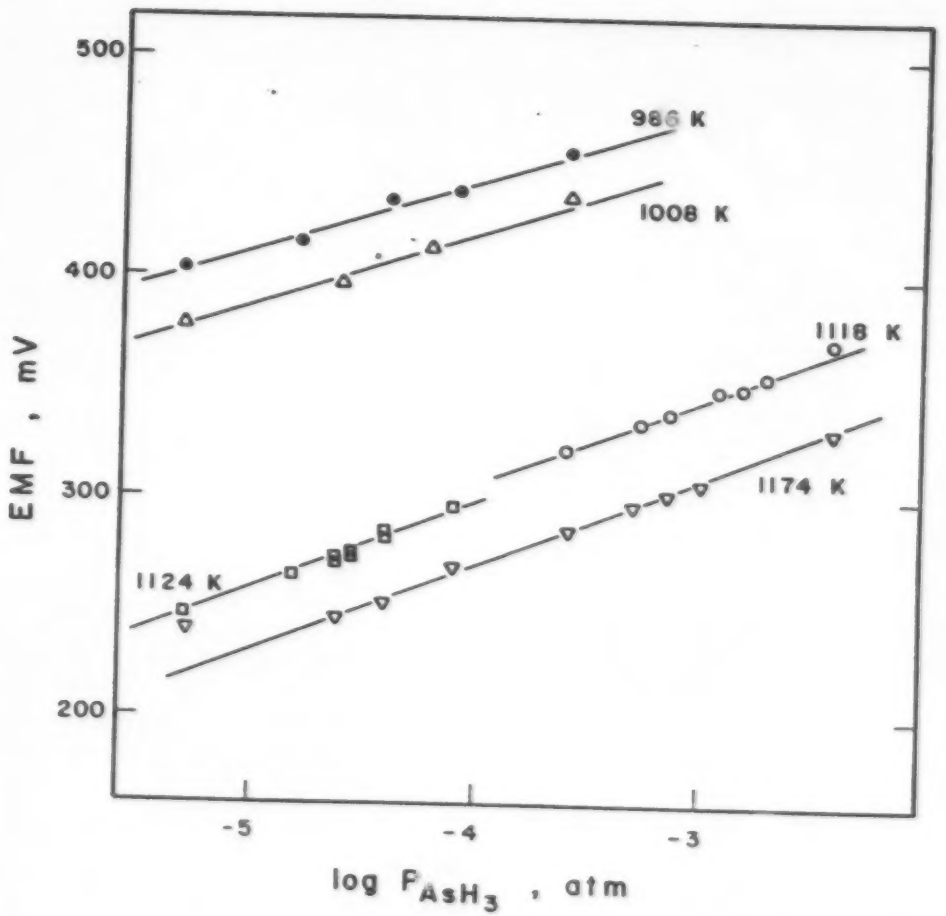

Figure 9: EMF as a function of log P_{AsH_3} [atm] for the Ag β-alumina electrolyte, sensor I, at 986°, 1008°, 1118°, 1124° and 1174° K and P_{O_2} = 0.21 atm

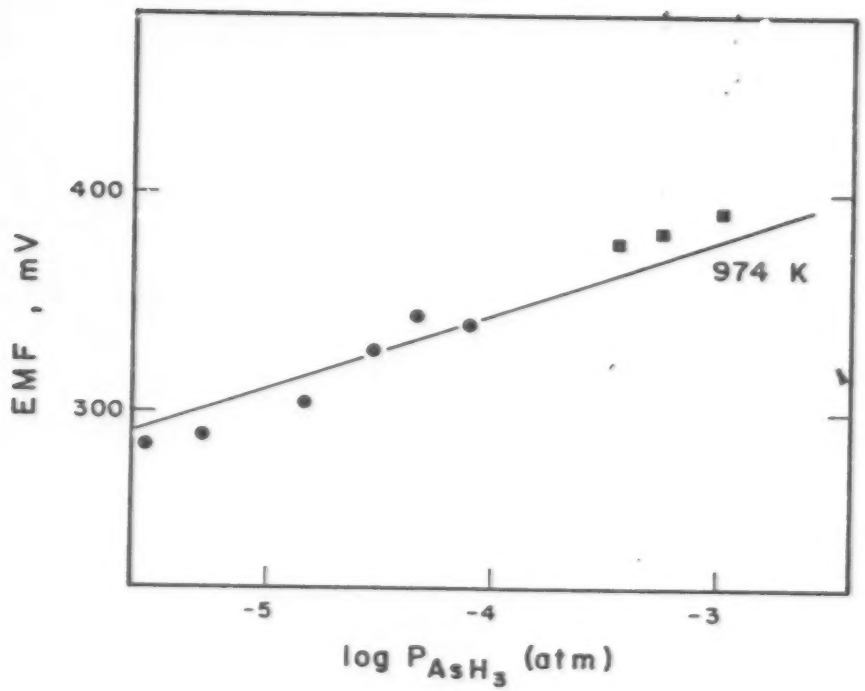

Figure 10: EMF as a function of log P_{AsH_3} [atm] for the Ag β-alumina electrolyte, sensor II, at 974°K and P_{O_2} = 0.21 atm: Flowrate: 0.5 ml/s

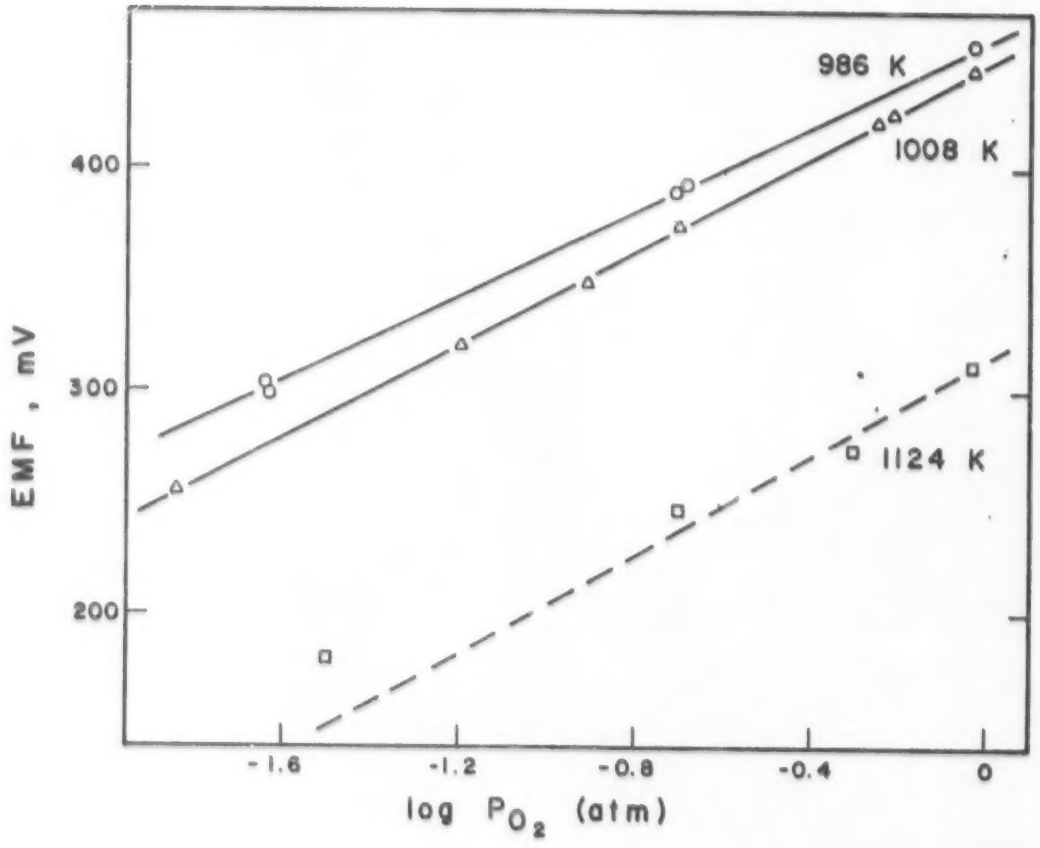

Figure 11: EMF as a function of log P_{O_2} [atm] for the Ag β-alumina electrolyte, sensor I, at P_{AsH_3} = 5.3 ppm and 986°, 1008° and 1124°K

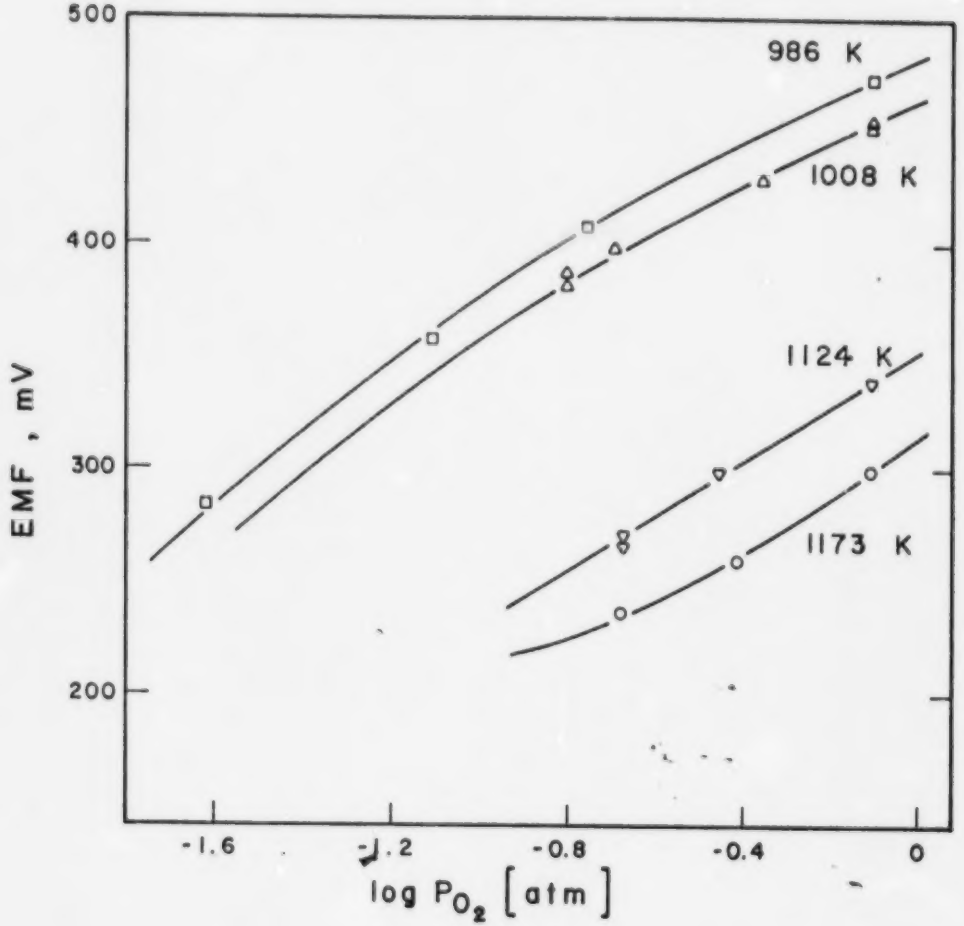

Figure 12: EMF as a function of log P_{O_2} [atm] for the Ag β-alumina electrolyte, sensor I, at P_{AsH_3} = 23 ppm and 986°, 1008°, 1124° and 1173°K

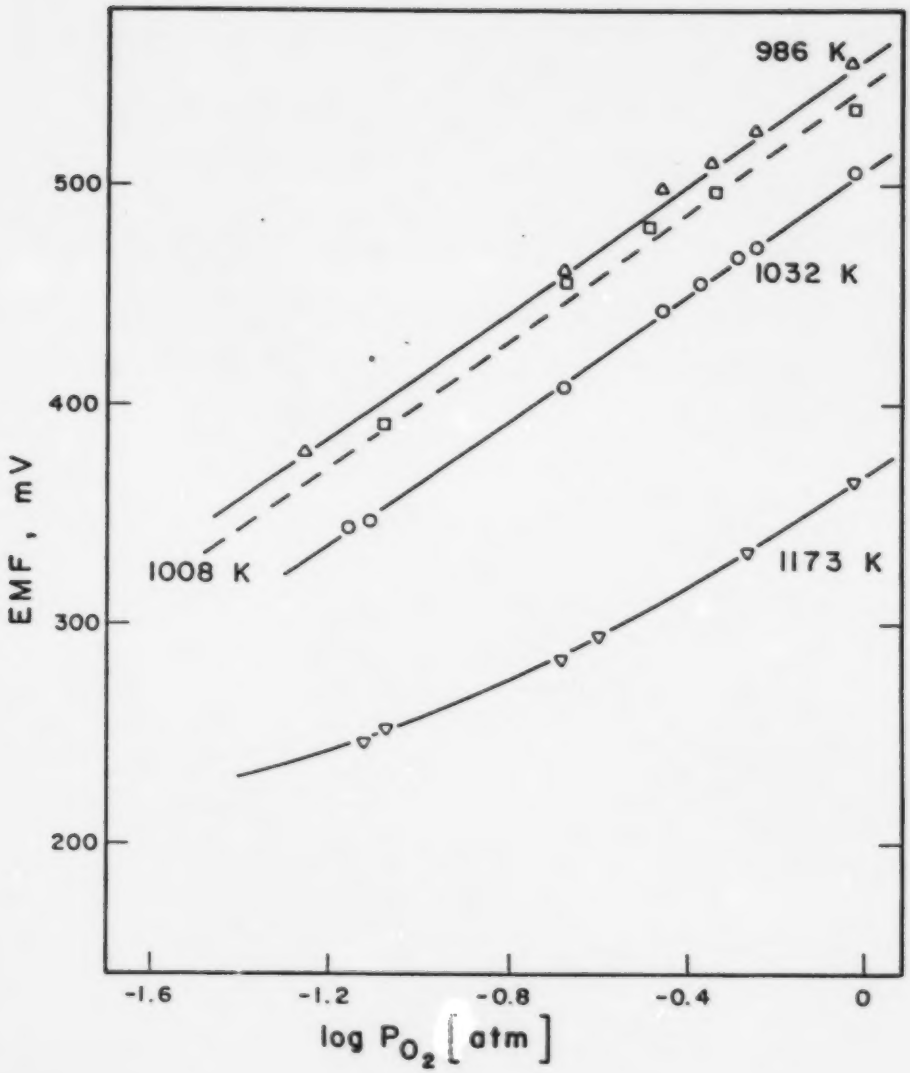

Figure 13: EMF as a function of log P_{O_2} [atm] for the Ag β-alumina electrolyte, sensor I for P_{AsH_3} = 255 ppm at 986°, 1008°, 1032° and 1173°K

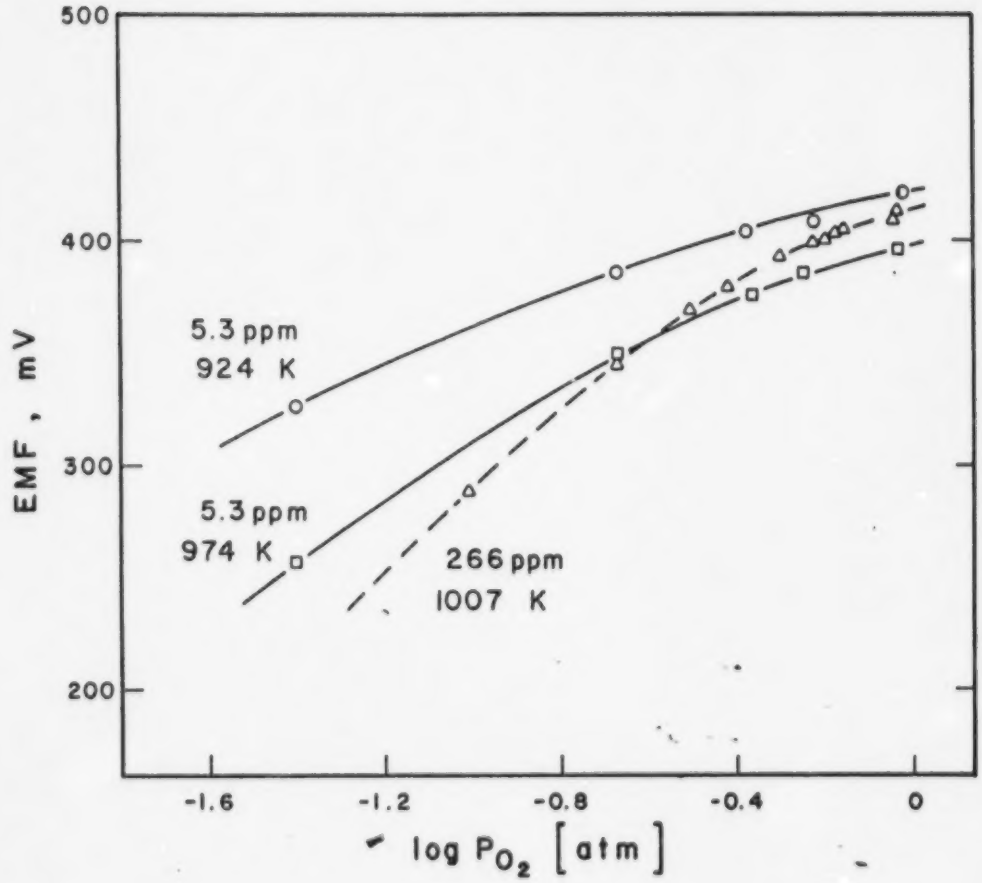

Figure 14: EMF as a function of log P_{O_2} [atm] for the Ag β-alumina electrolyte, sensor II, for P_{AsH_3} = 5.3 ppm at 924° and 974°K, and for P_{AsH_3} = 266 ppm and 1007°K

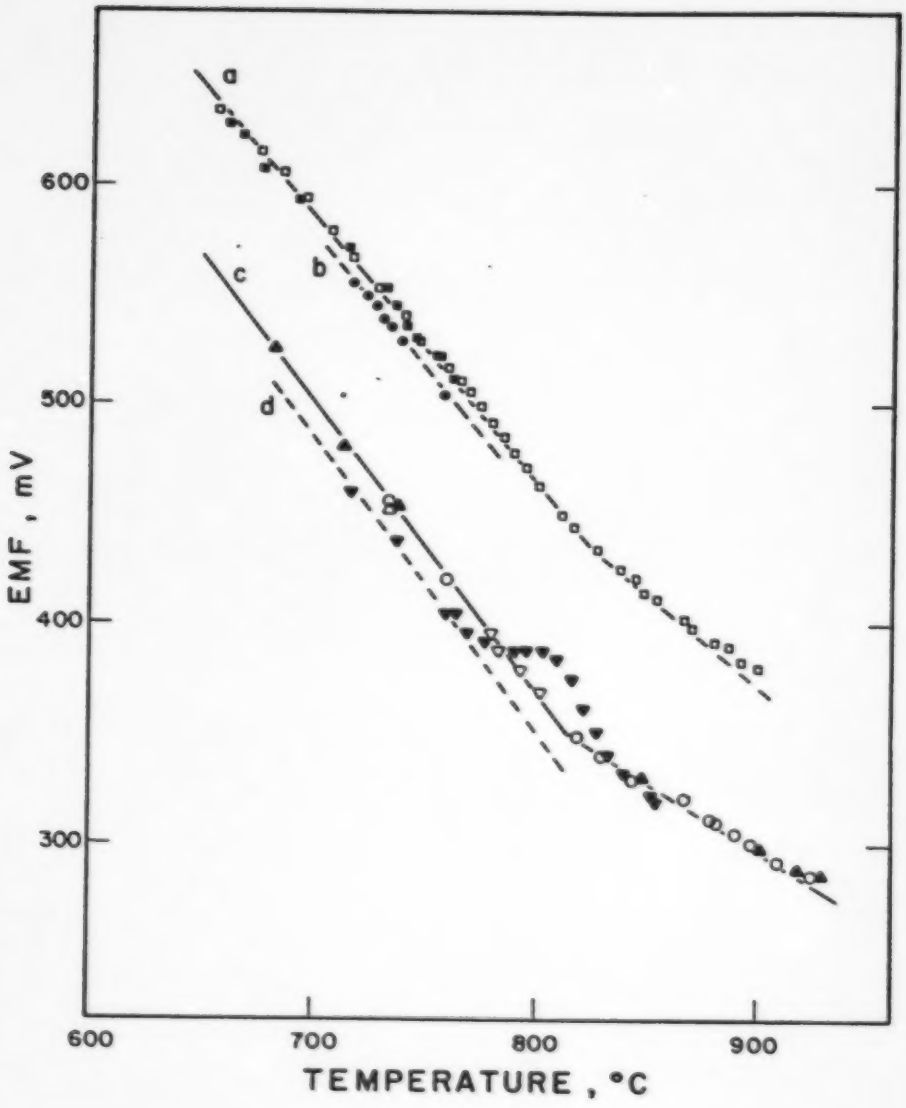

Figure 15

(Caption on following page).

Figure 15: EMF as a function of temperature for Ag β-alumina electrolyte, sensor I:

a) sensor I, P_{AsH_3} = 1847 ppm, P_{O_2} = 0.63 atm, flowrate = 0.15 ml/s: ■) heating, □) cooling ...

b) sensor I, P_{AsH_3} = 255 ppm, P_{O_2} = 0.95 atm, f.r. = 1 ml/s, heating .....

c) sensor I, P_{AsH_3} = 36 ppm, P_{O_2} = 0.63 atm, f.r. = 0.6 ml/s: ▲) heating, ○ , ▽) cooling ....

d) sensor I, P_{AsH_3} = 255 ppm, P_{O_2} = 0.21 atm, f.r. = 1 ml/s, cooling .....

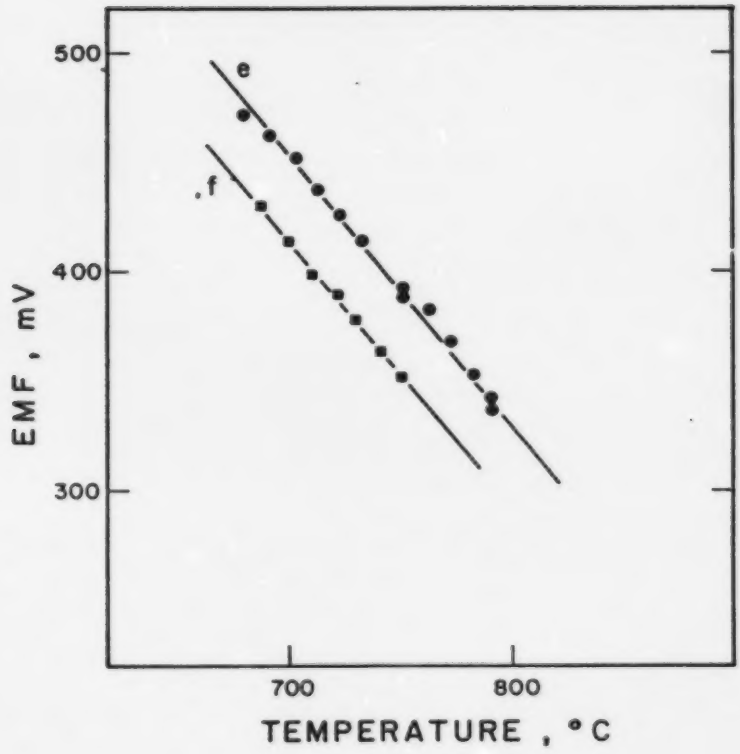

Figure 16: EMF as a function of temperature for the Ag β-alumina electrolyte, sensor II: e) P_{AsH_3} = 1847 ppm, P_{O_2} = 0.63 atm, flowrate = 0.15 ml/s; f) P_{AsH_3} = 36 ppm, P_{O_2} = 0.63 atm, flowrate 1 ml/s

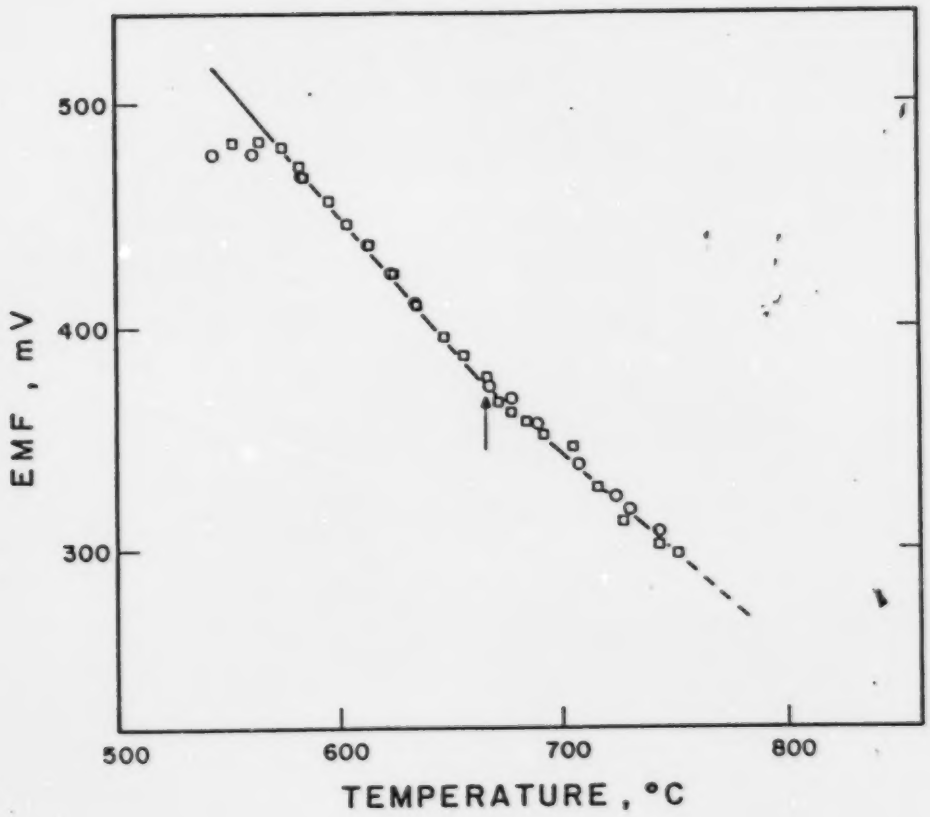

Figure 17: EMF as a function of temperature for the Ag β-alumina electrolyte, sensor II-2, $\tilde{P}_{As_4O_6}$ = 31.1 ppm, P_{O_2} = 0.21 atm, flowrate 0.5 ml/s
□) heating, ○) cooling

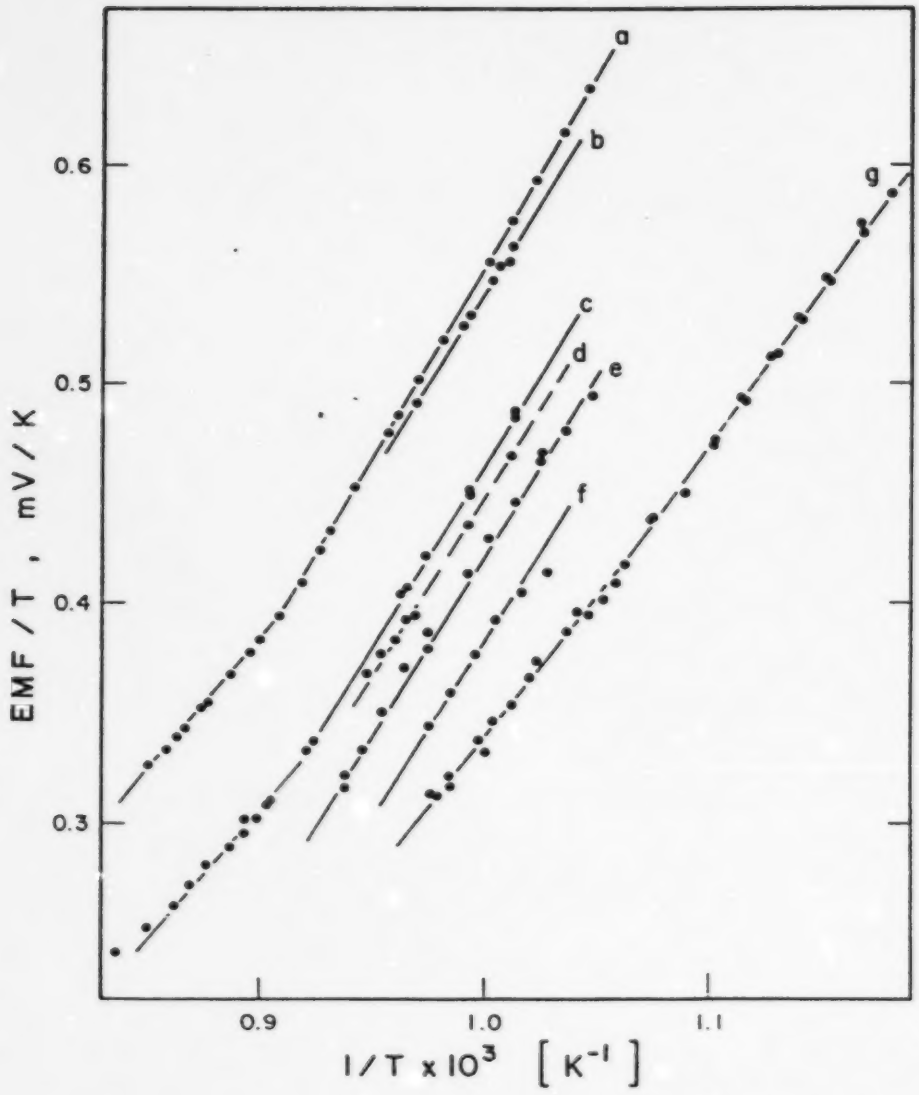

Figure 18

(Caption on following page).

Figure 18: EMF/T as a function of 1/T for the Ag β-alumina electrolyte:
a) sensor I, P_{AsH_3} = 1847 ppm, P_{O_2} = 0.63 atm, flowrate = 0.15 ml/s .....

b) sensor I, P_{AsH_3} = 255 ppm, P_{O_2} = 0.96 atm, f.r. = 1 ml/s .....

c) sensor I, P_{AsH_3} = 36 ppm, P_{O_2} = 0.63 atm, f.r. = 0.6 ml/s .....

d) sensor I, P_{AsH_3} = 255 ppm, P_{O_2} = 0.21 atm, f.r. = 1 ml/s .....

e) sensor II, P_{AsH_3} = 1847 ppm, P_{O_2} = 0.63 atm, f.r. = 0.15 ml/s .....

f) sensor II, P_{AsH_3} = 36 ppm, P_{O_2} = 0.63 atm, f.r. = 0.6 ml/s .....

g) sensor II-2, $\tilde{P}_{As_4O_6}$ = 31.1 ppm, P_{O_2} = 0.21 atm, f.r. = 0.5 ml/s .....

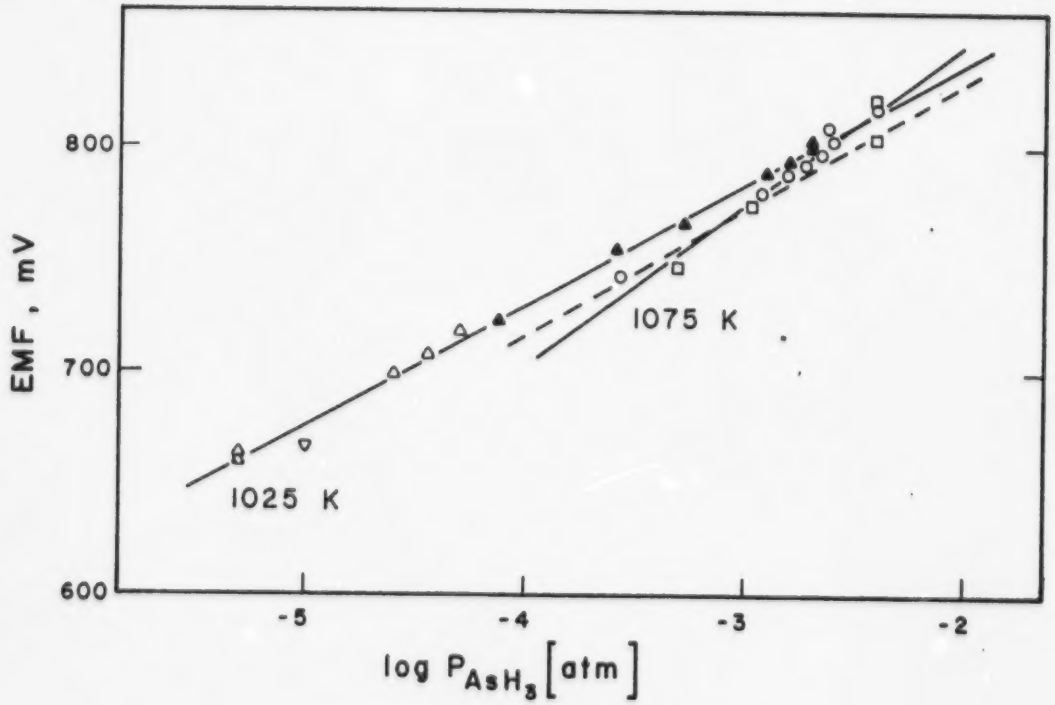

Figure 19: EMF as a function of log P_{AsH_3} [atm] for the sodium β-alumina electrolyte with air as a reference: at 1025°K, △) first set of data, ▲) second set of data; at 1075°K, □) first set, ○) second set of data

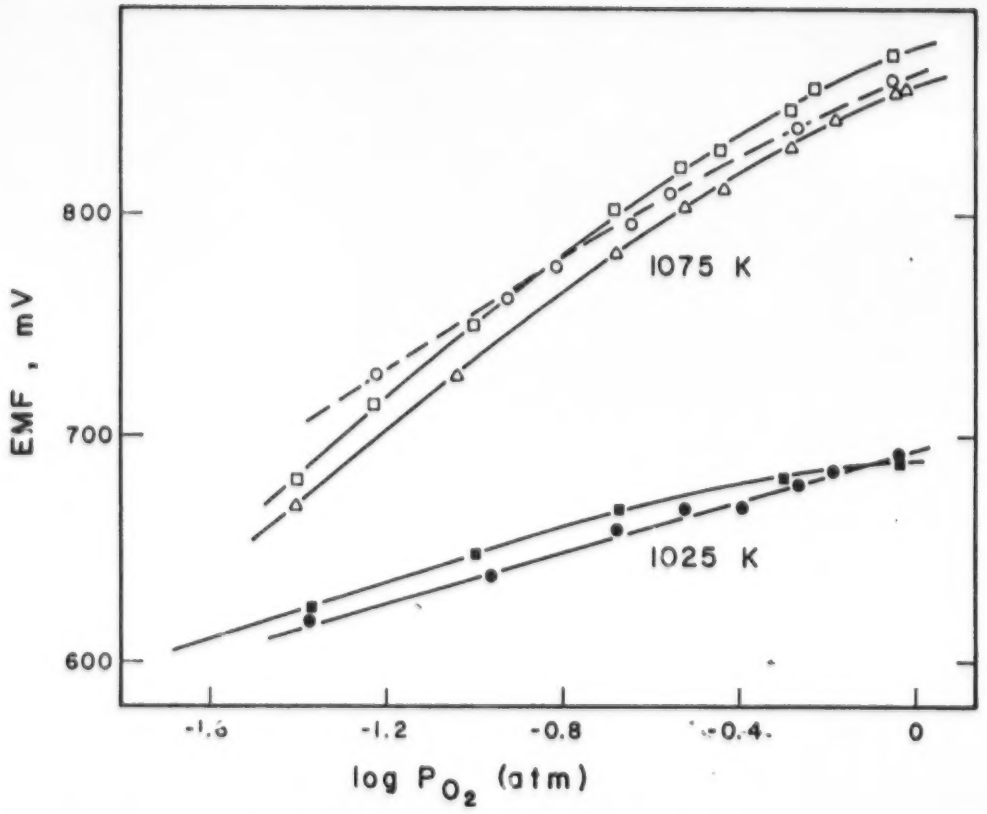

Figure 20: EMF as a function of log P_{O_2} [atm] for the sodium β-alumina electrolyte with air as a reference; △) 1075°K, P_{AsH_3} = 301 ppm, f.r. 1 ml/s; ○) 1075°K, P_{AsH_3} = 502 ppm, f.r. 0.5 ml/s; □) 1075°K, P_{AsH_3} = 502 ppm, f.r. = 1 ml/s; ●) 1025°K, P_{AsH_3} = 5 ppm, f.r. 1 ml/s; ■) 1025°K, P_{AsH_3} = 9.8 ppm, f.r. 1 ml/s

TABLE A.1

EXPERIMENTAL RESULTS FOR THE $AgZr_2(AsO_4)_3$ ELECTROLYTE

T [°K]	P_{AsH_3} [atm] × 10^6	P_{O_2} [atm]	FLOWRATE [ml/s]	EMF [mV]
886	83.8	0.162	2.05	375
	12	0.215	1.93	330
	8	0.219	2.00	323
	5.3	0.221	2.33	218
	3.4	0.223	2.67	302.5
	2.0	0.223	3.00	293.2
	1.8	0.222	3.40	295
	3.1	0.230	1.98	294
	3.5	0.223	2.67	301.4
	6.4	0.216	2.67	336
	84	0.161	2.00	369.5
	76.3	0.237	2.20	399.5
	71.3	0.287	2.42	408.3
	66.8	0.332	2.10	411.5
	61.9	0.381	1.82	406.4
	66.7	0.333	2.07	402.5
	71.3	0.287	2.40	398.7
	86.2	0.138	2.00	360.1
	91.2	0.097	1.90	328
	86.0	0.140	2.00	373.4
	84.4	0.156	2.02	383
	78.7	0.213	0.83	385
	55.2	0.775	1.00	384.8
	43	0.225	1.43	382
	23.6	0.210	2.65	375
	18.8	0.215	3.29	372.8
	15	0.211	4.13	369.4
	8.7	0.225	3.83	363.5
	5.8	0.233	3.71	353.9
	3.4	0.239	3.62	344.4

TABLE A.1 (Cont'd)

T [°K]	P_{AsH_3} [atm] × 10^6	P_{O_2} [atm]	FLOWRATE [ml/s]	EMF [mV]
886	1.7	0.222	3.45	327
	2.0	0.224	3.00	323
	83.7	0.163	2.05	374
	75	0.253	0.7	390.9
	28	0.719	0.93	406
	128.7	0.974	3.26	474
	251	0.95	3.5	461
	161.9	0.968	3.2	459.3
	1245	0.75	1.34	470.4
	937.3	0.814	1.16	490.3
	646.1	0.871	1.6	481.7
	624.4	0.876	1.6	490
	269.9	0.946	1.5	477
	252	0.191	2.35	463
	161	0.194	2.34	467
	131	0.198	2.31	460.5
	109	0.200	2.45	453.7
	87	0.203	2.46	451.7
	82.8	0.172	0.8	365
	73	0.264	0.6	396
	19.6	0.804	1.67	419
	116.7	0.977	3.45	467.9
	173.5	0.965	2.78	477
	87	0.983	3.45	465

TABLE A.2

EXPERIMENTAL DATA FOR THE $NaCa(AsO_4)$ ELECTROLYTE

Reference: arsenolite bath 111.3°C: $\tilde{P}_{As_4O_6}$ = 1.3 ppm, flowrate: 1.25 ml/s

T [°K]	P_{AsH_3} [atm] × 10^6	P_{O_2} [atm]	FLOWRATE [ml/s]	EMF [mV]
1075	77.7	0.207	1.255	200
	91.4	0.068	1.255	173
	95.5	0.017	1.339	115
	2.8	0.967	1.216	238
	8.2	0.916	1.244	249
	15.8	0.839	1.255	267
	32.1	0.672	1.220	263
	71.6	0.195	1.335	218
	92	0.056	1.240	162
	95.4	0.017	1.313	116
	7.5	0.194	1.364	179
	29.8	0.146	1.350	188
	46.9	0.109	1.295	179
	62.2	0.077	1.165	166.3
	76.4	0.046	1.316	144.2
	76.4	0.046	1.316	151.9
	91.4	0.016	1.315	109.9

TABLE A.2 (Cont'd)

T [°K]	P_{AsH_3} [atm] × 10^6	P_{O_2} [atm]	FLOWRATE [ml/s]	EMF [mV]
949	95.4	0.008	1.325	183.8
	90.5	0.015	1.235	225.2
	75.8	0.047	1.305	284.6
	60.4	0.079	1.120	305
	47.0	0.109	1.252	319.4
	27.1	0.152	1.314	332
	49.6	0.104	1.283	320
	92.1	0.013	1.254	219
	73.8	0.052	1.217	279.9
	77.3	0.210	1.280	351
	96	0.019	1.315	228.4
	90.3	0.075	1.265	297.6
	77.2	0.212	1.224	342.6
	62.6	0.358	1.033	366.7
	31.0	0.684	1.111	379
	77.8	0.206	1.206	340

TABLE A.2 (Cont'd)

T [°K]	P_{AsH_3} [atm] × 10^6	P_{O_2} [atm]	FLOWRATE [ml/s]	EMF [mV]
1017	8.1	0.917	1.206	382.6
	2.8	0.972	1.175	368
	31.0	0.684	1.205	380
	63.3	0.354	1.068	345
	77.8	0.206	1.260	327.4
	92.1	0.071	1.259	286.4
	95.4	0.018	1.312	211.9
	29.2	0.702	1.174	375
	50.3	0.487	1.170	367
	6.6	0.194	1.380	289.7
	92.3	0.011	1.283	188.9
	76.0	0.047	1.290	263.3
	45.1	0.113	1.210	298.1
	28.2	0.150	1.326	307.2
	2.5	0.205	1.415	276
	47.8	0.108	1.230	297.9
	27.8	0.150	1.281	302.6
	62	0.077	1.146	276.6
	71	0.058	1.265	271.7
	76	0.047	1.290	262
	94	0.014	1.492	205.3

TABLE A.3

EXPERIMENTAL RESULTS FOR THE Ag β-ALUMINA ELECTROLYTE, SENSOR I, EMF CONCENTRATION DEPENDENCE

T [°K]	P_{O_2} [atm]	P_{AsH_3} [atm] × 10^6	-log P_{AsH_3} [atm]	EMF [mV]
986	0.21	5.3	5.276	402.8
		5.3	5.276	401.6
		15	4.824	414.9
		78.6	4.105	441
		36.6	4.437	426.7
		5	5.301	395
		304	3.517	461
1008		5.3	5.276	378.5
		23.5	4.629	399.0
		78.3	4.105	415.3
		266	3.575	457
		5	5.301	374.5
1118		5.3	5.276	246
		23	4.629	267
		28.5	4.545	270
		40.2	4.396	281
		77.6	4.111	295.5
1124		15.2	4.815	265.5
		252.3	3.600	322.5
		536	3.271	334.5
		692.4	3.160	338.2
		1184	2.927	343
		1503	2.823	349
		1958	2.708	353
		3966	2.402	358

TABLE A.3 (Cont'd)

T [°K]	P_{O_2} [atm]	P_{AsH_3} [atm] × 10^6	-log P_{AsH_3} [atm]	EMF [mV]
1174	0.21	23.5	4.621	246.3
		37.6	4.424	252.3
		77.6	4.111	270.0
		5.3	5.290	250.7
		5	5.301	244
		266	3.580	285.4
		3966	2.402	331.4
		501	3.290	296.6
		711	3.148	302.2
		1040	2.985	307.8
		1526	2.816	316.7
		1895	2.722	318.8

TABLE A.3 (Cont'd)

T [°K]	P_{AsH_3} [atm] × 10^6	P_{O_2} [atm]	-log P_{O_2} [atm]	EMF [mV]
986	5.3	0.95	0.022	456.7
		0.21	0.678	395
		0.20	0.699	390
		0.023	1.638	302.8
1008	5.3	0.95	0.022	444
		0.614	0.212	425.3
		0.563	0.249	421.8
		0.122	0.915	347
		0.062	1.206	320
		0.014	1.845	256
1124	5.3	0.95	0.022	309
		0.509	0.293	270.4
		0.03	1.493	180
		0.21	0.678	247

TABLE A.3 (Cont'd)

T [°K]	P_{AsH_3} [atm] × 10^6	P_{O_2} [atm]	-log P_{O_2} [atm]	EMF [mV]
986	23	0.76	0.119	473.1
		0.168	0.775	408.5
		0.078	1.108	358
		0.023	1.638	284
1008	23	0.160	0.796	382
		0.782	0.102	453.2
		0.79	0.101	458
		0.162	0.789	385.4
		0.157	0.803	383
		0.436	0.361	430
		0.200	0.699	399
1124	23	0.768	0.115	340
		0.347	0.460	299
		0.211	0.677	267
		0.211	0.677	270
1173	23	0.770	0.115	300.6
		0.372	0.429	262.1
		0.207	0.683	246.0

TABLE A.3 (Cont'd)

T [°K]	P_{AsH_3} [atm] × 10^6	P_{O_2} [atm]	-log P_{O_2} [atm]	EMF [mV]
986	255	0.95	0.022	555.4
		0.207	0.683	461.9
		0.053	0.273	377.6
		0.347	0.460	497.6
		0.450	0.347	511.6
		0.427	0.370	514.3
		0.571	0.243	524.9
		0.604	0.219	523.3
1008		0.95	0.022	535
		0.450	0.347	496
		0.340	0.467	482.1
		0.207	0.683	457.1
		0.082	0.084	392
1032		0.95	0.022	508.2
		0.56	0.252	473
		0.069	0.169	342.0
		0.076	0.119	338
		0.203	0.692	408.1
		0.34	0.470	444.1
		0.428	0.369	455.6
		0.520	0.284	467.8
1073		0.95	0.022	367.4
		0.538	0.270	330.7
		0.252	0.598	294.5
		0.207	0.683	285.4
		0.084	1.076	252.2
		0.075	1.123	245.6

TABLE A.4

EXPERIMENTAL DATA FOR THE Ag β-ALUMINA ELECTROLYTE, SENSOR I, EMF TEMPERATURE DEPENDENCE

P_{AsH_3} [atm] × 10^6	P_{O_2} [atm]	FLOWRATE [ml/s]	T [°K]	EMF [mV]
1857	0.63	0.15	1174	382.6
			1164	387.9
			1158	392.9
			1153	394.9
			1143	402.1
			1139	404.6
			1127	413.8
			1116	422.0
			1111	426.2
			1100	435.1
			1089	445.2
			1084	450.4
			1178	457.3
			1073	464.6
			1067	472
			1062	479.4
			1051	493.0
			1045	499.5
			1039	505.6
			1030	517.7
			1019	529.6
			1009	541
			998	553.1
			988	566.2
			978	579.6
			967	594.0
			956	606.1
			946	616.6
			935	629.1
			926	633.2

TABLE A.4 (Cont'd)

P_{AsH_3} [atm] × 10^6	P_{O_2} [atm]	FLOWRATE [ml/s]	T [°K]	EMF [mV]
1857	0.63	0.15	939	624.3
			947	607.1
			962	602.6
			977	589.5
			989	574.2
			988	577.3
			1007	543
			1008	547.3
			1009	546.3
			1014	541.8
			1022	532.1
			1028	524.1
			1033	516.4
255	0.95	1.0	988	555.2
			990	550
			994	550.2
			998	546.4
			1003	538.6
			1009	530.5
			1032	506
			1007	535
			1007	531

TABLE A.4 (Cont'd)

P_{AsH_3} [atm] × 10^6	P_{O_2} [atm]	FLOWRATE [ml/s]	T [°K]	EMF [mV]
36	0.63	0.6	1006	452.1
			1006	454.1
			1006	456.0
			986	481.2
			986	479.4
			1006	454.9
			1026	432.5
			1039	420.3
			1082	364
			1082	367
			1085	361.2
			1035	421.6
			1105	343.8
			1118	336
			1118	333
			1141	320
			1141	323.9
			1151	313
			1163	306
			1174	299.3
			1184	292.2
			1175	296.9
			1196	288
			1050	403.1
			1057	397.2
			1060	391.1
			1068	380
			1074	371.1
			1095	353.8
			1065	386
			1035	421.6

TABLE A.4 (Cont'd)

P_{AsH_3} [atm] × 10^6	P_{O_2} [atm]	FLOWRATE [ml/s]	T [°K]	EMF [mV]
255	0.21	1.0	1031	406.6
			1035	407.1
			1042	398.7
			1049	396
			1055	389
			1061	390.7
			1068	390.6
			1075	389.8
			1082	386.4
			1089	377.9
			1095	363.7
			1100	355.0
			1108	342.4
			1113	335.3
			1120	331.8
			1126	324

TABLE A.5

EXPERIMENTAL RESULTS FOR THE Ag β-ALUMINA ELECTROLYTE, SENSOR II, EMF CONCENTRATION DEPENDENCE

T [°K]	P_{O_2} [atm]	P_{AsH_3} [atm] × 10^6	-log P_{AsH_3} [atm]	EMF [mV]
974	0.21	5.0	5.300	287
		2.8	5.553	286.6
		13.9	4.856	302.2
		28.4	4.547	329
		42.6	4.371	343.5
		77.4	4.111	338
		325	3.488	376.4
		533	3.273	380.1
		919	3.037	386.3

T [°K]	P_{O_2} [atm]	P_{AsH_3} [atm] × 10^6	-log P_{O_2} [atm]	EMF [mV]
924	0.21	5.3	0.678	385
	0.04		1.398	323.1
	0.420		0.377	403.6
	0.600		0.222	408.1
	0.95		0.022	420.8
974	0.95	5.3	0.022	396.7
	0.56		0.250	385.5
	0.425		0.372	375.7
	0.21		0.678	349
	0.04		1.398	256.6
1007	0.95	266	0.022	414.8
	0.60		0.222	399.8
	0.50		0.301	393.9
	0.37		0.432	379
	0.29		0.513	368
	0.21		0.678	342
	0.10		1.000	284
	0.95		0.022	409.6

TABLE A.6

EXPERIMENTAL RESULTS FOR THE Ag β-ALUMINA ELECTROLYTE, SENSOR II, EMF TEMPERATURE DEPENDENCE

P_{AsH_3} [atm] $\times 10^6$	P_{O_2} [atm]	FLOWRATE [ml/s]	T [°K]	EMF [mV]
1857	0.63	0.15	954	471.5
			965	462.1
			976	456.9
			986	437.7
			996	426.2
			1007	415.3
			1026	388
			1026	396.2
			1037	383.8
			1047	366.1
			1057	351.6
			1064	336
			1064	342
			976	452
36	0.63	0.6	973	403.7
			984	398.3
			995	390.2
			1004	377.8
			1015	365.4
			1025	353.0

TABLE A.7

EXPERIMENTAL RESULTS FOR THE Ag β-ALUMINA ELECTROLYTE, SENSOR II-2, EMF TEMPERATURE DEPENDENCE

$\tilde{P}_{As_4O_6}$ [atm] × 10^6	P_{O_2} [atm]	FLOWRATE [ml/s]	T [°K]	EMF [mV]
31.1	0.21	0.5	1016	306
			1003	318.9
			997	323.6
			981	338.1
			962	361.5
			951	366.9
			940	373.2
			907	410.5
			897	422.2
			887	437.6
			856	467
			835	477
			816	477
			824	483.6
			839	483.6
			849	480.9
			854	472.4
			856	468.4
			869	457.6
			877	446.2
			887	437.4
			897	421.8
			908	410
			920	394.8
			930	389.5
			933	389.2
			939	378.4
			945	366.8
			951	361.4
			957	357.1
			966	352.3
			979	346.9
			989	328.7
			997	311.3
			1015	300.5
			1025	298.5

TABLE A.8

EXPERIMENTAL RESULTS FOR THE Na β-ALUMINA ELECTROLYTE

T [°K]	P_{O_2} [atm]	P_{AsH_3} [atm] × 10^6	-log P_{AsH_3} [atm]	EMF [mV]
1075	0.21	3966	2.402	817
		2380	2.620	809.4
		2368	2.626	800.7
		2178	2.662	795.9
		1908	2.720	791.2
		1623	2.790	787.6
		1255	2.900	777.9
		262	3.580	741.1
		3976	2.400	799
		994	2.960	771
		502	3.299	745.8
1025	0.21	1908	2.719	803
		1580	2.801	791
		1255	2.901	785
		502	3.299	766
		502	3.299	765
		266	3.575	753
		77	4.113	721
		46	4.337	717
		36	4.444	707
		24	4.620	698.6
		5.3	5.276	662
		5.0	5.301	658
		9.8	5.009	666
		77	4.113	726
		1900	2.721	798

TABLE A.8 (Cont'd)

FLOWRATE [ml/s]	T [°K]	P_{AsH_3} [atm] × 10^6	P_{O_2} [atm]	-log P_{O_2} [atm]	EMF [mV]
1	1075	502	0.90	0.046	870.5
			0.575	0.232	854.2
			0.53	0.276	845.7
			0.40	0.400	827.5
			0.295	0.530	819.9
			0.21	0.678	800.7
			0.10	1.000	747.7
			0.04	1.398	682.3
0.5	1075	502	0.89	0.050	854
			0.52	0.284	834
			0.28	0.553	807
			0.21	0.678	788.2
			0.15	0.824	773.2
			0.06	1.222	728
1	1075	301	0.95	0.022	856.6
			0.90	0.046	852.6
			0.65	0.187	841.2
			0.53	0.276	828.1
			0.365	0.438	808
			0.295	0.530	803.3
			0.21	0.678	780.5
			0.095	1.022	712.0
			0.04	1.398	670.3

TABLE A.8 (Cont'd)

T [°K]	P_{AsH_3} [atm] × 10^6	P_{O_2} [atm]	-log P_{O_2} [atm]	EMF [mV]
1025	5	0.045	1.345	618
		0.109	0.961	637.8
		0.210	0.678	658.2
		0.280	0.548	661
		0.420	0.377	668.3
		0.550	0.260	678.6
		0.66	0.180	681.6
		0.90	0.046	690.0
1025	9.8	0.90	0.046	687.6
		0.61	0.215	681.1
		0.51	0.292	679
		0.30	0.523	667.7
		0.21	0.678	662.5
		0.21	0.678	665.8
		0.10	1.000	647.5
		0.045	1.345	623.6